REPORT DOCUMENTATION PAGE

Form Approved
OMB No. 0704-0188

1. REPORT DATE	2. REPORT TYPE	3. DATES COVERED *(From - To)*
24 August 2020	Technical Paper	17 August 2020 - 31 August 2020

4. TITLE AND SUBTITLE
DEVELOPMENT OF A NORMAL SHEAR STRESS AND TEMPERATURE (NSST) SENSOR CALIBRATION RIG

5a. CONTRACT NUMBER
FA9300-19-C-0003

5b. GRANT NUMBER

5c. PROGRAM ELEMENT NUMBER

6. AUTHOR(S)
Franklin Wong and James Fillerup

5d. PROJECT NUMBER

5e. TASK NUMBER

5f. WORK UNIT NUMBER
Q1Y8

7. PERFORMING ORGANIZATION NAME(S) AND ADDRESS(ES)
Micron Instruments
4509 Runway St.
Simi Valley, CA 93063

8. PERFORMING ORGANIZATION REPORT NUMBER

9. SPONSORING/MONITORING AGENCY NAME(S) AND ADDRESS(ES)
Air Force Research Laboratory (AFMC)
AFRL/RQRM
4 Draco Drive
Edwards AFB, CA 93524-7160

10. SPONSOR/MONITOR'S ACRONYM(S)

11. SPONSOR/MONITOR'S REPORT NUMBER(S)
AFRL-RQ-ED-TP-2020-183

12. DISTRIBUTION/AVAILABILITY STATEMENT
Distribution Statement A: Approved for Public Release; Distribution is Unlimited. PA Clearance Number: 20362; Clearance Date: 23 August 2020.

13. SUPPLEMENTARY NOTES
The U.S. Government is joint author of the work and has the right to use, modify, reproduce, release, perform, display, or disclose the work.

14. ABSTRACT
Development of shear stress sensors for solid propellant rocket motors was attempted in the early 1970's. The sensors needed large strains in the sensing elements to obtain sufficiently high signal-to-noise ratios for the foil strain gages that were used. With the availability of high performance semiconductor strain gages, it is possible to design not only a compact shear stress sensor, it is possible to design a sensor that can simultaneously measure the shear and normal stress components acting on a solid rocket motor bondline. The objective of this study is to design a calibration rig for a diaphragm-based normal shear stress and temperature (NSST) sensor. In this report, the design of a 'milling machine' type NSST calibration rig is presented. Preliminary tests evaluating the ability of the calibration rig to apply pure normal and pure shear to the NSST sensor show that the calibration rig applies the loading boundary conditions to the NSST sensor in a manner that is consistent with the boundary conditions used in the NSST sensor finite element analysis. Moreover, the experimentally measured NSST normal and shear bridge outputs were comparable, in relative magnitude, to the predicted NSST normal and shear bridge outputs thereby validating the modeling technique employed and the results obtained in the finite element analysis. Four prototype NSST sensors were built. Three of the prototype sensors were calibrated using the NSST calibration rig. The calibration results are presented.

15. SUBJECT TERMS
N/A

16. SECURITY CLASSIFICATION OF:			17. LIMITATION OF ABSTRACT	18. NUMBER OF PAGES	19a. NAME OF RESPONSIBLE PERSON
a. REPORT	b. ABSTRACT	c. THIS PAGE			James Singleton
Unclassified	Unclassified	Unclassified	SAR	71	19b. TELEPHONE NUMBER *(Include area code)* N/A

DEVELOPMENT OF A NORMAL SHEAR STRESS AND TEMPERATURE (NSST) SENSOR CALIBRATION RIG

Design and Validation

FC Wong
JM Fillerup

Micron Instruments
4509 Runway St.
Simi Valley, CA 93063

August 2020

Micron Instruments

Contract Report

Micron CR 2020-002

This work was performed at Micron Instruments between January 2020 and July 2020 for Contract FA9300-19-C-0003, Subtopic 5 Sensor Technology Development for Solid Rocket Motors under Broad Agency Announcement Motor Aging and Surveillance Technology (BAA MAST) Call 3 (BAA-RQR-2014-0002) Aging and Surveillance (A&S) Technology Development.

Abstract

Development of shear stress sensors for solid propellant rocket motors was attempted in the early 1970's. The sensors needed large strains in the sensing elements to obtain sufficiently high signal-to-noise ratios for the foil strain gages that were used. With the availability of high performance semiconductor strain gages, it is possible to design not only a compact shear stress sensor, it is possible to design a sensor that can simultaneously measure the shear and normal stress components acting on a solid rocket motor bondline. The objective of this study is to design a calibration rig for a diaphragm-based normal shear stress and temperature (NSST) sensor. In this report, the design of a 'milling machine' type NSST calibration rig is presented. Preliminary tests evaluating the ability of the calibration rig to apply pure normal and pure shear to the NSST sensor show that the calibration rig applies the loading boundary conditions to the NSST sensor in a manner that is consistent with the boundary conditions used in the NSST sensor finite element analysis. Moreover, the experimentally measured NSST normal and shear bridge outputs were comparable, in relative magnitude, to the predicted NSST normal and shear bridge outputs thereby validating the modeling technique employed and the results obtained in the finite element analysis. Four prototype NSST sensors were built. Three of the prototype sensors were calibrated using the NSST calibration rig. The calibration results are presented.

Table of contents

List of Figures

List of Tables

Acknowledgements

The authors would like to acknowledge the support from James Singleton, Group Lead – SRM Aging and Surveillance, Solid Rocket Motors Branch, AFRL Aerospace Systems Directorate, Edwards AFB.

The authors would also like to thank our colleagues at Micron Instruments, Danny Evans for the prototype Normal Shear Stress and Temperature (NSST) sensor wiring plan and Paul Kim and Robin Raedeke for gaging the NSST sensors. The guidance provided by Herbert Chelner concerning sensor compensation and testing is gratefully acknowledged.

This page intentionally left blank.

1. INTRODUCTION

Failure at the propellant-to-liner or liner-to-case interface at or near the stress relief termination is one of the major failure modes in a solid propellant rocket motor [1]. Numerical methods and polymeric material characterization techniques have been developed to handle stress singularities and nonlinear behavior. The presence of intentional and non-intentional material discontinuities, irregular component geometries and material variability, though, makes numerical assessment of the stress state in a production motor more complicated. Instrumenting all or a sample of motors with normal-shear stress sensors would allow the bondline stress state to be measured in critical, high risk areas thereby increasing confidence that the stress state acting on the bondline is known. Both these items are important for accurate determination of the remaining rocket motor service life.

Micron has modified the design of its Dual Bond Stress and Temperature (DBST) sensor to measure shear stress as well as normal stress [2]. The optimal geometry of the Normal Shear Stress and Temperature (NSST) fixture comprised of two end-tabs sandwiching a polymer cylinder that is temporarily bonded to the NSST sensor was determined to be:

a) thickness of the polymer on top of the sensor to the loading surface diameter ratio = 1,
b) loading surface diameter to the sensor diameter ratio = 3,
c) sensor diameter = 0.30 in.
d) diaphragm diameter of the sensor = 0.15 in.
e) diaphragm thickness = 0.0055 in.

The objective of the present work is to design a calibration rig that applies normal and shear loads individually or in combination with the constraint that the two end-tabs must remain parallel for all applied force loading angles.

This report documents the development of the NSST calibration rig design and its validation. Section 2 summarizes the requirements of calibration rig as determined by the results in [2]. Section 3 discusses the calibration rig concepts and the design of the concept that was chosen. Section 4 describes the fabrication of the NSST sensor. Section 5 presents the results of the preliminary tests that determine whether the calibration rig applies the loading conditions on the NSST as required. Section 6 presents the calibration results for the prototype NSST sensors.

2. BACKGROUND

The Micron Dual Bond Stress and Temperature (DBST) sensor currently incorporates one strain gage bridge to measure diaphragm deformations corresponding to normal stresses. Micron proposed that an additional strain gage bridge be incorporated onto the sensor diaphragm to simultaneously measure deformations related to shear stress [2]. The Normal Shear Stress and Temperature (NSST) sensor design was developed using the linear elastic finite element analysis (FEA) method.

The starting point for the finite element analysis leveraged off the work done by AMRDEC in 2006 to model a bond strength test specimen. Micron calls the bond strength test specimen customized for the NSST sensor a 'NSST fixture'. A no-rotation constraint is imposed on the top end-tab to better control the displacement field applied to the NSST fixture both numerically and experimentally. Thus, the top end-tab always remains parallel to the lower end-tab no matter what forces are applied to the top end-tab. Figure 1 shows the expected deformation and diaphragm strains when such a boundary condition is imposed on the NSST sensor.

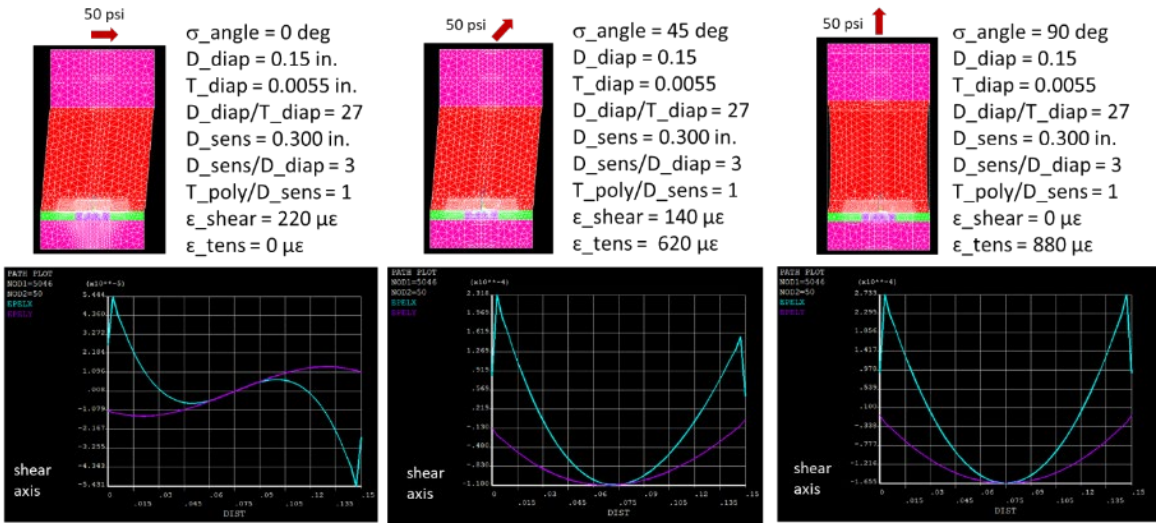

Figure 1: Theoretical NSST diaphragm strains for no end-tab rotation and applied force boundary conditions.

Figure 2 illustrates the required force-displacement boundary conditions that need to be applied to the top end-tab to generate the diaphragm strains shown in Figure 1. Any NSST calibration rig design must be able to accurately apply these boundary conditions. Note that the applied force is listed as Force/2 because a half-model was used in the finite element analysis. A NSST calibration rig should be able to apply twice the listed force.

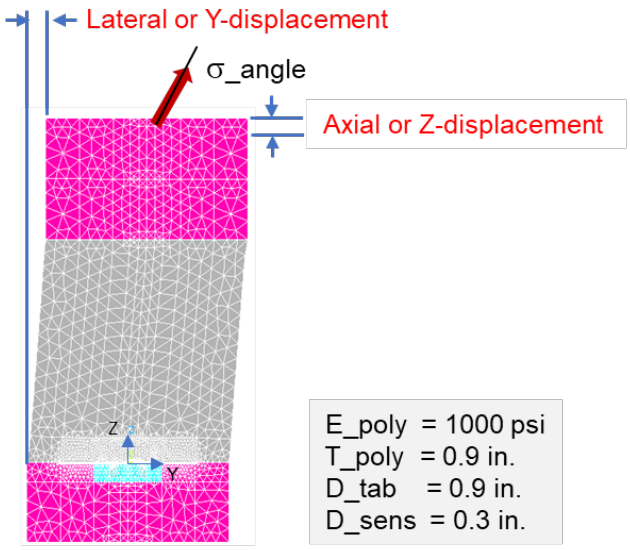

Angle	Y-displacement / Force/2	Z-displacement / Force/2
0 deg (shear)	0.213 in. / 15.9 lbs 5.4 mm / 70 N	-0.11e-4 in / 0 lbs 0.3 mm / 0 N
45 deg (tens-shear)	0.151 in. / 11.24 lbs 3.9 mm / 50 N	0.029 in. / 11.24 lbs 0.8 mm / 50 N
90 deg (tension)	0 in. / 0 lbs 0 mm / 0 N	0.041 in. / 15.9 lbs 1 mm / 70 N

Figure 2: Design Displacements and Forces (F/2) for NSST Calibration Rig.

3. CALIBRATION RIG AND NSST FIXTURE DESIGN

This Section discusses the concepts examined for the calibration rig design, the selection of commercially available components for the rig, the design of secondary structures needed to complete the calibration rig and the selection of the temporary adhesive needed to bond the NSST diaphragm to the NSST fixture.

3.1 Concepts

Three concepts are proposed for the NSST calibration rig. Each concept is evaluated against the three criteria: 1) boundary condition accuracy, 2) manufacture difficulty, and 3) overall cost.

The mechanical linkage, Concept no. 1 (see Figure 3), assumes that a tensile test machine is available to apply a vertical displacement on the calibration rig and measure the resultant uniaxial force. The angle of the applied displacement relative to the vertical axis of the NSST fixture is adjusted by tilting the base of the rig to the desired angle. The rig uses a horizontally constrained frame to impose a vertical motion relative to the NSST fixture's vertical axis (Z-direction) and a vertically constrained shuttle to impose a horizontal motion relative to the fixture's horizontal axis (Y-direction). Figure 2 lists displacements in the range from 0.0001 to 0.213 in. (0.3 to 5.4 mm). Normal machining accuracy is 0.004 in. (0.1 mm). With these small displacements, it is difficult to imagine how part tolerances can be tightened such that hysteresis and backlash effects can be well controlled. The cost of this concept however would be relatively low if a tensile test machine is readily available.

The hexapod, Concept no. 2 (see Figure 4), is a high accuracy multi-degree of freedom device. It can easily maintain a no-rotation boundary condition on an end-tab while applying the required displacements to impose the desired force vector. For example, the PI H-825 [3] is able to generate a 30 lbs force (150 N) in any direction with an incremental motion resolution of 0.00001 in. (0.3 micron), a backlash of 0.0001 in. (3 micron) and a repeatability of +/- 0.00002 (0.5 micron). A 3-axis load cell would need to be mounted on the hexapod platform to measure the force vector. The hexapod with loadcell would need to be mounted in a rigid frame so that the NSST fixture is held in place between the frame and loadcell. The frame and component tolerances would need to be well controlled. A complete NSST calibration rig would be comprised of a hexapod, the drive electronics to command the six leg displacements, a 3-axis loadcell and a data acquisition system to capture the loadcell data. The cost of such a system would be quite high given the number of high precision devices and electronics.

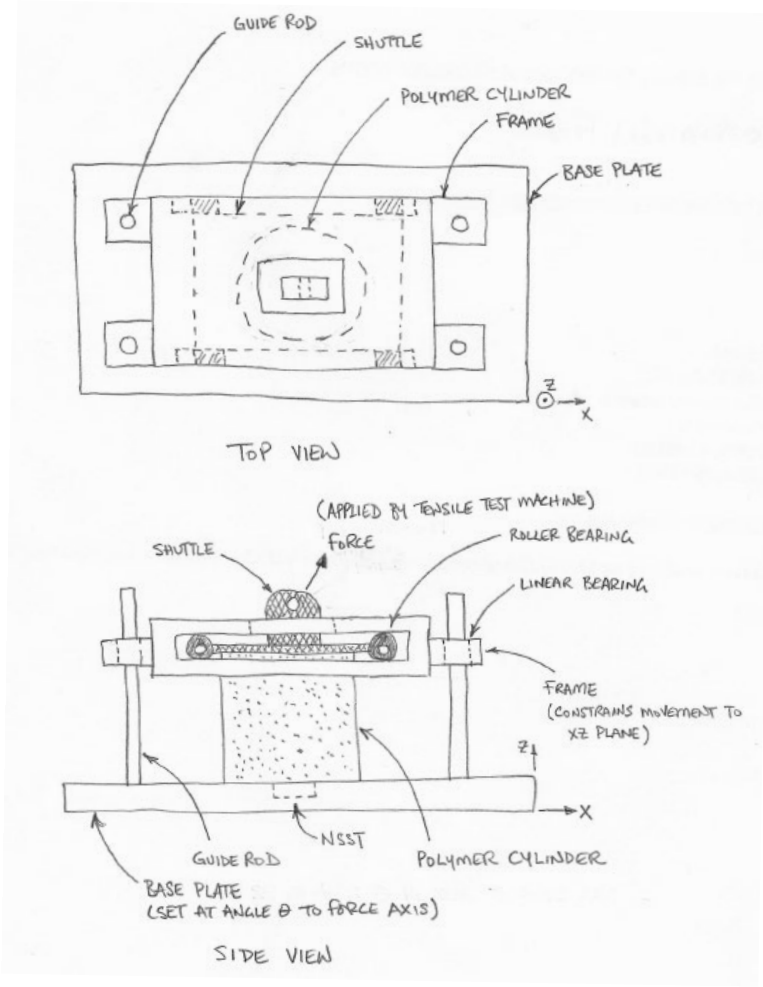

Figure 3: Concept No. 1 - Mechanical Linkage Concept.

Figure 4: Concept No. 2 - Six-Axis Hexapod Concept.

The milling machine, Concept no. 3 (see Figure 5), exploits the characteristics of commercially available milling machines. These tools accurately translate a work piece in three-axes using high precision linear actuators. The frame of a milling machine is typically designed to be rigid to minimize frame distortions when tool forces are applied to the work piece. The NSST fixture would be mounted between the tool head that is mounted on the stage of a vertically oriented linear actuator and a loadcell which is mounted on the stage of a horizontally oriented linear actuator. The horizontal and vertical displacements listed in Figure 2 would be applied by the independent motion of the linear actuators. Measurement of a force vector would need a data acquisition system and a 3-axis loadcell that is mounted on the workpiece platform. The difficulty of manufacturing a milling machine concept would be relatively low because the precision is available in commercial linear actuators. Positioning the linear actuators accurately relative to one another should be possible using standard machining tolerances. The cost of this system would be higher than the mechanical linkage concept and lower than the hexapod concept.

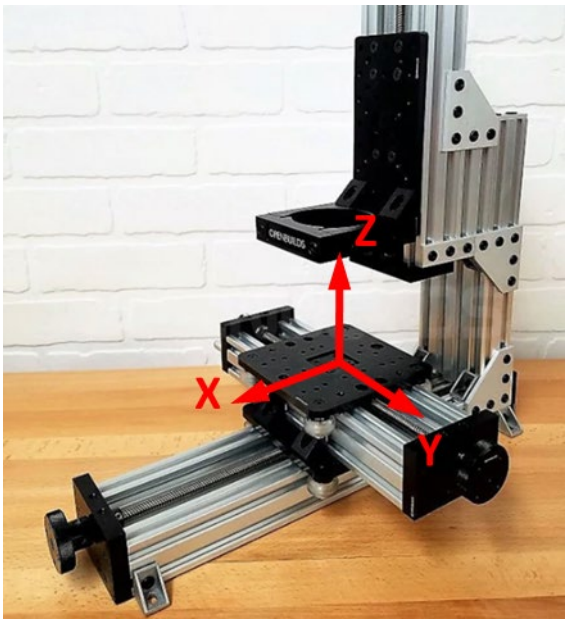

Figure 5: Concept No. 3 - Milling Machine Concept.

Table 1 summarizes the factors discussed in the preceding paragraphs. The mechanical linkage Concept no. 1 has a high risk of not functioning correctly because it requires high part tolerances to minimize backlash and hysteresis. The hexapod Concept no. 2 has the mechanical performance that is needed, however, its cost is quite high. The milling machine Concept no. 3 appears to have the right proportion of displacement accuracy and precision and relative ease of manufacture at a reasonable cost.

Table 1. Comparison of Factors leading to NSST Calibration Rig Concept Selection

Concept	Boundary Condition Accuracy	Manufacture Difficulty	Overall Cost
1. Mechanical Linkage	low	high	low
2. Hexapod	high	medium	high
3. Milling Machine	high	low	medium

Based on these factors, it was decided to proceed with the detailed design of a NSST calibration rig using the milling machine concept.

3.2 YZ-Stage Component Selection

The success of the milling machine concept rests on the selection of the linear actuators. Nook Industries Inc. has a large range of screw-driven modular actuators [4]. After consultation with an application engineer, the ELK 30 actuator was selected. The general characteristics of the ELK 30 actuator are given in Table 2 [5]. The model number code of the ELK 30 actuator selected for the calibration rig is given in Annex A.

Table 2. ELK 30 linear actuator characteristics

Parameter	Value
Cross-section size (mm x mm)	30 x 30
Screw (dia mm – mm advance per turn)	8-2.5
Screw type	Ball screw
Stage width (mm)	70
Stage length (mm)	82
Total length (mm)	160
Fx static max (N)	750
Fy static max (N)	90
Fz static max (N)	90
Mx static max (Nm)	12
My static max (Nm)	12
Mz static max (Nm)	15
Elastic modulus (N/mm^2)	70000

The maximum displacements shown in Section 2, Figure 2 range from 0.3 mm to 5.4 mm. Therefore, to have sufficient displacement resolution, a lead screw that advances only a short distance for each revolution of the shaft is required. The shortest lead distance shaft that Nook Industries manufactures is 2.5 mm per revolution. So, we would expect to rotate the shaft from 43.2 deg to 2 revolutions and 144 deg to obtain the calculated displacements. The ball screw type has low friction to aid with the smooth application of displacements.

The load needs to be monitored as the displacements are applied in the Y and Z axes. A three-axis force load cell from Interface Inc. was selected. The characteristics of the Model 3A120 3-axis load cell with 200 N capacity is provided in Table 3 [6].

Table 3. Model 3A120 3-axis load cell characteristics

Parameter	Value
Nonlinearity (% FS)	± 0.2
Hysteresis (% FS)	± 0.02
Crosstalk YZ (%)	2
Rated capacity any axis (N/lbf)	200/45
Deflection Y (mm/in)	0.06/0.002
Deflection Z (mm/in)	0.12/0.005

3.3 YZ-Stage Component Design

Nook Industries provides a tool called the Modular Calculator to calculate the safety factor for the expected loads and moments on an ELK actuator [7]. This tool was used to verify that the recommended ELK 30 was able to handle the expected loads.

The maximum expected loads were shown in Section 2, Figure 2. The loads were increased by 10 N and used in the design loads shown in Table 4.

Table 4. Design loads for NSST calibration rig

Load Case	Value
1. Normal force only (N/lbf)	150/34
2. Shear force only (N/lbf)	150/34
3. Combined Normal and Shear Normal force (N/lbf) Shear force (N/lbf)	 110/25 110/25

Figures 6 and 7 illustrate the three load cases as they act on the horizontal stage called the Y-Stage and the vertical stage called the Z-Stage. The coordinate systems shown in the figures correspond to the coordinates used by the Nook Modular Calculator.

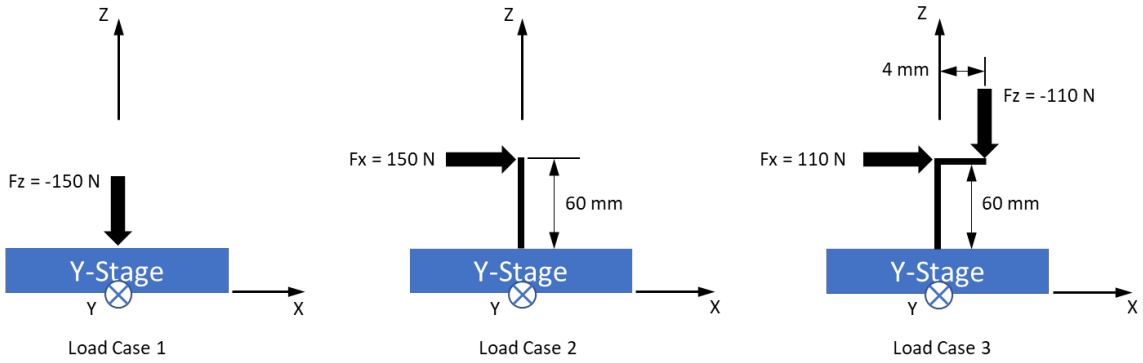

Figure 6: Load cases for Y-Stage in Nook coordinate axes.

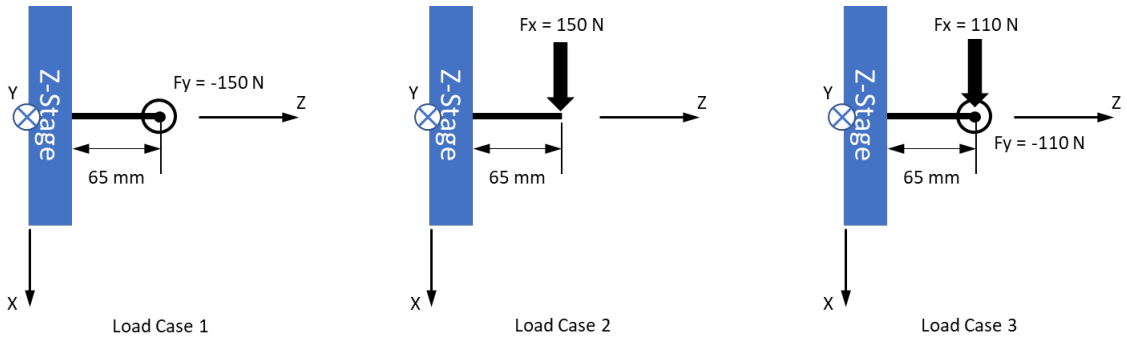

Figure 7: Load cases for Z-Stage in Nook coordinate axes.

The results from the Modular Calculator for the six load cases are shown in Table 5. As seen, all safety factors are positive. Load case 3 on the Z-Stage is the most severe.

Nook Industries provides Equation 1 to estimate of the actuator lateral deflection for the Y-Stage Load Case 1 assuming the ends of the actuator are built-in [8].

$$f = \frac{FL^3}{192 \cdot E \cdot I} \tag{1}$$

where f is lateral deflection (mm), F is the load (150 N), L is the total actuator length (280 mm), E is the actuator modulus (70E3 N/mm^2) and I is the actuator moment of inertia (4E4 mm^4).

The estimated actuator lateral deflection for the values provided is 0.003 mm which is acceptable compared to the applied displacements.

Table 5. Safety factor results for Nook actuators

Stage	Load Case	Safety Factor
Y	1. Fz = -150 N	5.6
	2. Fx = 150 N @ 60 mm	2.3
	3. Fx = 110 N @ 60 mm, Fz = -110 N @ 4 mm	3.0
Z	1. Fy = 150 N @ 65 mm	1.4
	2. Fz = 150 N @ 65 mm	2.1
	3. Fx = 110 N @ 65 mm, Fy = -110 N @ 65 mm	1.1

3.4 YZ-Stage Supporting Structure

Selection of the linear actuator and load cell allowed the structure to support these components to be designed. The purpose of the supporting structure is to hold the components in the proper geometric relationship with the NSST fixture. Figure 8 shows the full assembly of the NSST calibration rig and the identification of the linear actuator, 3-axis load cell and the NSST fixture.

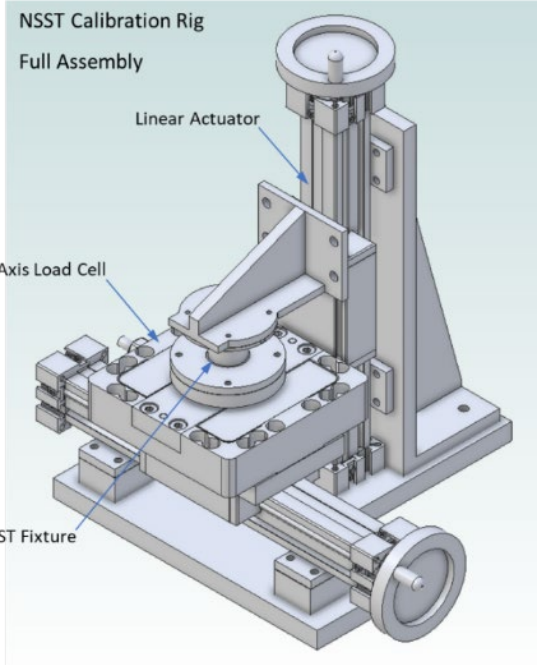

Figure 8: Full assembly of NSST calibration rig.

Figure 9 highlights the different components making up the supporting structure. Dimensioned drawings of each component are provided in Annex A.

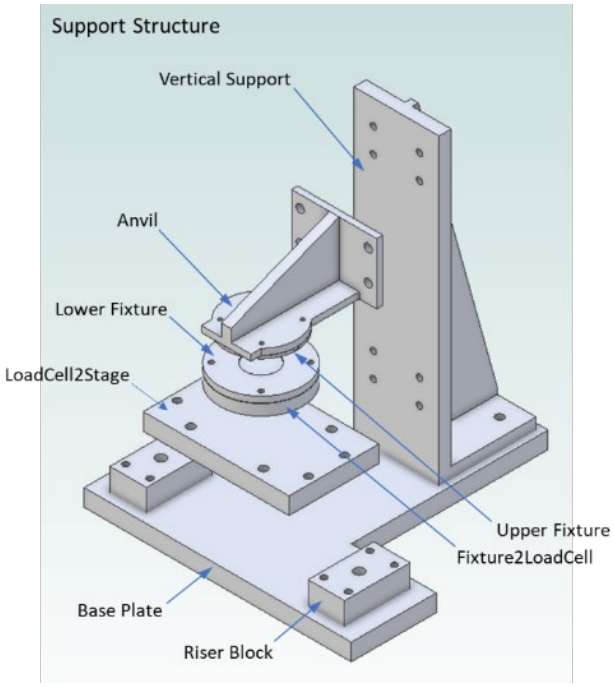

Figure 9: Supporting structure for NSST calibration rig.

3.5 Analysis of Z-Stage Supporting Structure

The Vertical Support and the Anvil in Figure 9 bear the vertical and horizontal forces acting on the NSST fixture. A finite element analysis was carried out using the Mecway program [9] on the imported STL files for the Vertical Support and Anvil to verify that the tip displacements were within acceptable levels. Best practice methods were employed in the modeling, meshing and analysis [10].

The forces acting on the Anvil are shown in the three load cases in Figure 7. The loads are transmitted to the Anvil through four bolts in the 'Upper Fixture'. The total force was evenly divided and applied to the four bolted connection points in the model. The Anvil is supported by a bolted connection to the Z-Stage through four bolts. The regions around the bolt holes were assigned a fully fixed boundary condition.

Graphical results of the analysis are shown in Figure 10. Table 6 lists the maximum vector displacement for each load case. The designator 'C' has been added to the force nomenclature to signify that the combined normal-shear forces are different than the normal only and shear only forces. Note that the Anvil coordinate system is oriented differently than the coordinate system used for the Nook actuator analysis. As Table 6 shows, a maximum vector displacement of 0.030 mm occurs under combined normal-shear loading (Load Case 3) when the Anvil is fabricated from Al 6061-T6. The maximum displacements are at acceptable levels when compared to the applied displacements.

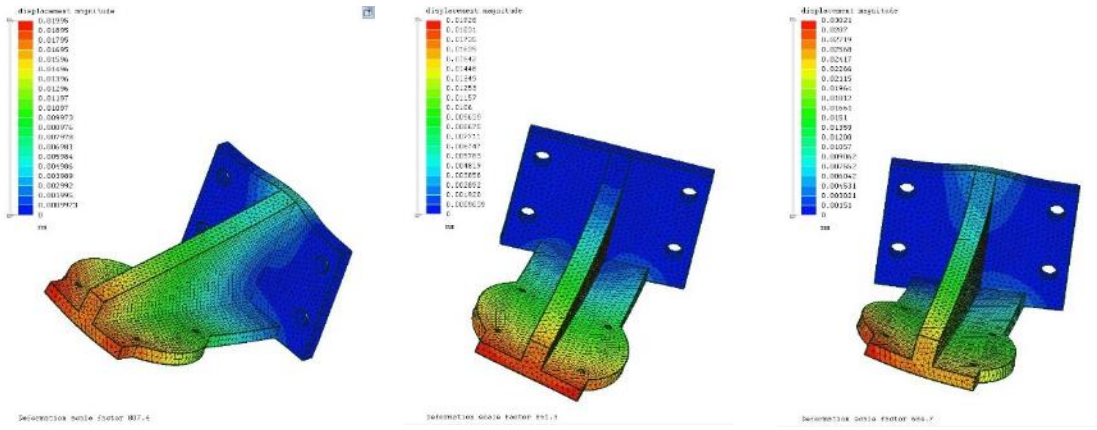

Figure 10: Anvil deformations for normal, shear and normal-shear load cases.

Table 6. Anvil maximum vector displacements

Load Case	Max Amplitude (mm)
1. Fy = 150 N	0.020
2. Fz = 150 N	0.019
3. FyC = 110 N, FzC = 110 N	0.030

The forces acting on the Vertical Support are shown in Figure 11. The forces Fx1, Fx2, Fx3 and Fx4 acting on the four Vertical Support bolt holes are a result of the Anvil forces Fy and Fz (values from Figure 7) acting across moment arms of DX and DZ. The coordinate system in Figure 11 matches the coordinate system used in the finite element model of the Vertical Support.

Equation 2 was used to calculate the bolt hole reaction force, Feqv1, for Load Case 1 (normal force only). The directions of the bolt hole forces are assigned by inspection and given in Table 7.

$$Fy \cdot DX = Feqv1 \cdot [2(DH - DM) + 2(DM - DL)] \quad (2)$$

Equation 3 was used to calculate the bolt hole reaction force, Feqv2, for Load Case 2 (shear force only). The directions of the bolt hole forces are assigned by inspection and given in Table 7.

$$-Fz \cdot DX = Feqv2 \cdot 4 \cdot DZ \quad (3)$$

The bolt hole forces for Load Case 3 (normal-shear forces) are the sum of the bolt hole forces for normal and shear loads. The equations for the bolt hole forces are shown in Table 7. Note that the designator ‘C’ has been added to the nomenclature to signify that the combined normal-shear forces are different than the normal only and shear only forces.

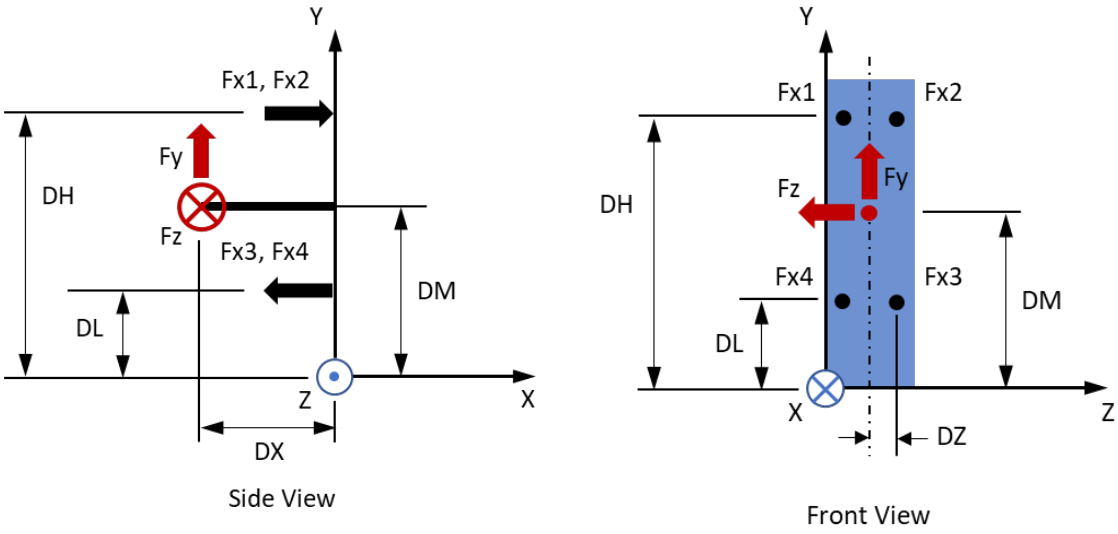

Figure 11: Conversion of Anvil forces to Vertical Support forces

Table 7. Vertical Support bolt hole force equations for Load Cases 1 to 3

Load Case	Fx1	Fx2	Fx3	Fx4
1. Fy	+Feqv1	+Feqv1	-Feqv1	-Feqv1
2. Fz	+Feqv2	-Feqv2	-Feqv2	+Feqv2
3. FyC, FzC	+Feqv1C +Feqv2C	+Feqv1C -Feqv2C	-Feqv1C -Feqv2C	-Feqv1C +Feqv2C

The values for the parameters shown in Figure 11 are given in Table 8. The moment arms are taken from the dimensions of the supporting structure components (see Annex A). The numerical values for the bolt hole forces are given in Table 9.

Table 8. Vertical Support load case parameters

Forces	Value	Distances	Value
Fy (normal only) (N/lbf)	150/34	DH (mm/in)	220/8.66
Fz (shear only) (N/lbf)	150/34	DL (mm/in)	60/2.36
FyC (normal-shear) (N/lbf)	110/25	DX (mm/in)	112/4.41
FzC (normal-shear) (N/lbf)	110/25	DM (mm/in)	153/6.02
---	---	DZ (mm/in)	19/0.75

Table 9. Vertical Support bolt hole force values for Load Cases 1 to 3

Load Case	Fx1 (N/lbf)	Fx2 (N/lbf)	Fx3 (N/lbf)	Fx4 (N/lbf)
1. Fy = 150 N/34 lbf	+38.5/+8.73	+38.5/+8.73	-38.5/-8.73	-38.5/-8.73
2. Fz = 150 N/34 lbf	+162/+36.7	-162/-36.7	-162/-36.7	+162/+36.7
3. FyC = 110 N/25 lbf, FzC = 110 N/25 lbf	+201/+45.6	-123/-45.6	-201/-45.6	+123/+45.6

The bolt hole forces from Table 9 were applied in a finite element model of the Vertical Support. The displacements in the bolt hole regions on the base were set to zero. Figure 12 shows the vector displacement contours and Table 10 provides the maximum vector displacements.

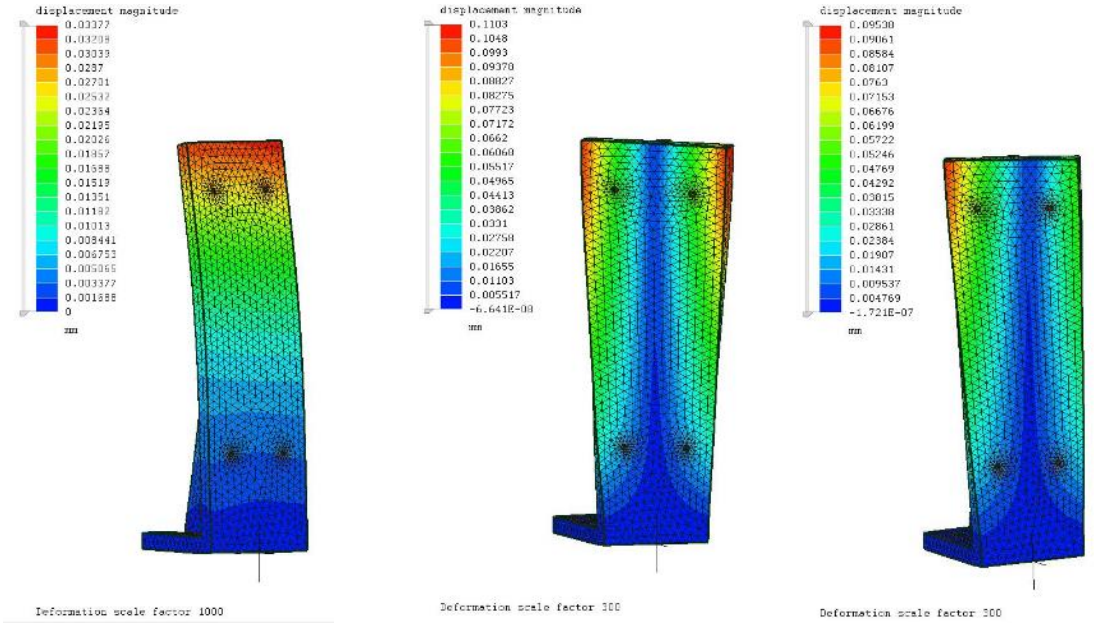

Figure 12: Vertical Support deformations for normal, shear and normal-shear load cases.

Table 10. Vertical Support maximum vector displacements

Load Case	Max Amplitude (mm)
1. Fy = 150 N	0.034
2. Fz = 150 N	0.110
3. FyC = 110 N, FzC = 110 N	0.095

A maximum vector displacement of 0.110 mm occurs under the 'shear only', Load Case 2, when the Vertical Support is fabricated from Al 6061-T6. The vector displacements are at acceptable levels when compared to the applied displacements.

3.5 NSST Polymer Selection

The finite element analysis of the NSST fixture in [2] showed that the sensor diaphragm would deform as desired under normal and shear loads as long as the modulus of the polymer cylinder was below 3200 psi or 22 MPa.

A source for bulk neoprene was found [11]. Since rubbery materials are difficult to machine, the sheet material was purchased with a thickness as close as possible to the ideal 0.9 in. thickness [2]. The characteristics of two neoprene materials are given in Table 11.

The range of moduli shown for each Shore A was estimated using the information from [12], [13]and [14]. For the Shore 60A neoprene, the moduli ranged from 320 psi to 520 psi (2.2 MPa to 3.6 MPa). For the Shore 70A neoprene, the moduli ranged from 390 psi to 910 psi (2.7 MPa to 6.3 MPa). The finite element analyses in [2] assumed a polymer modulus of 1000 psi (6.99 MPa) or roughly 1.1 times the highest neoprene modulus. If the highest modulus neoprene material was used, we would expect that the applied displacements in the NSST calibration rig to be roughly 1.1 times greater than that shown in the Table contained in Figure 2.

Table 11. Characteristics of Polymer Material

Material	Shore A	Thickness (mm/in)	Modulus (MPa/psi)
Neoprene	60	25.3/1.00	2.2 to 3.6/320 to 520
Neoprene	70	26.0/1.03	2.7 to 6.3/390 to 910

To create the cylindrical shape, a hammer-driven circular punch with a diameter of 15/16 in. or 0.9375 in. (23.8 mm) was used [15]. The punch was mounted in a press and drawn down into the neoprene sheet to create the polymer cylinder. A photo of a typical cylinder is shown in Figure 13. The cylinder has more of an hourglass shape than a right cylinder

shape due to the thickness of neoprene the punch had to cut through. The dimensions of the fabricated cylinders are provided in Table 12.

Figure 13: NSST fixture punched polymer cylinder

Table 12. Dimensions of Neoprene Cylinders

Specimen	Shore A	Thickness (mm/in)	End Diameter (mm/in)	Middle Diameter (mm/in)
N60-1	60	25.3/1.00	23.7/0.93	20.7/0.82
N60-2	60	25.3/1.00	23.7/0.93	20.7/0.82
N60-3	60	25.4/1.00	23.7/0.93	20.7/0.82
N70-1	70	26.0/1.03	23.6/0.93	21.3/0.84
N70-2	70	26.0/1.03	23.6/0.93	21.2/0.83
N70-3	70	26.1/1.03	23.6/0.93	21.2/0.83

3.6 NSST Adhesive Selection

The NSST fixture is comprised of five components: 1) lower fixture (end-tab), 2) polymer cylinder, 3) upper fixture (end-tab), 4) NSST sensor to be calibrated, and 5) double-sided tape (see Figure 14). The double-sided tape plays a critical role because it must transfer the displacements from the YZ-stages through the upper and lower fixtures, the polymer cylinder and onto the NSST diaphragm. The upper and lower fixtures are made from 4140 steel to minimize part distortion as the loads are transferred through the bolted connections. The adhesive on the double-sided tape must be compatible with steel and the polymer which in this case is neoprene.

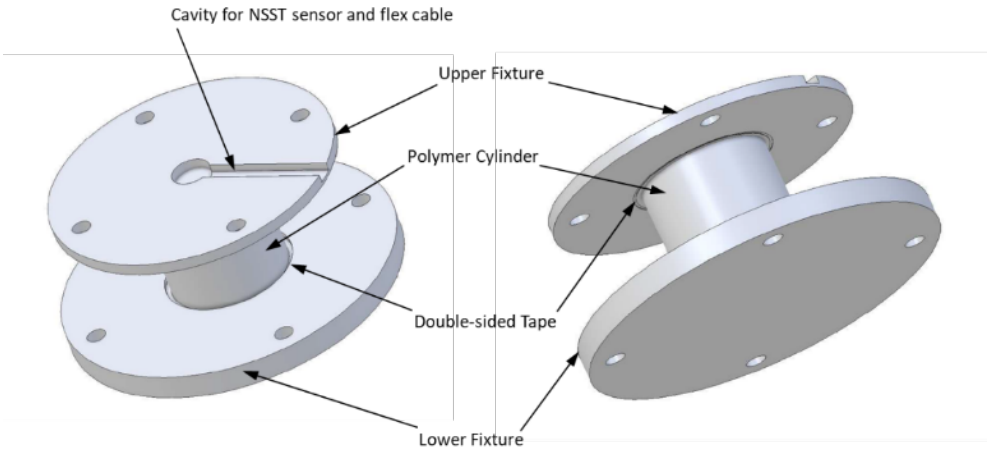

Figure 14: NSST fixture components

The adhesive on the lower fixture double-sided tape connecting the Polymer Cylinder and the Lower Fixture can be formulated for a permanent bond since it is not necessary to separate these two components. The adhesive on the upper fixture double-sided tape connecting the upper fixture and the NSST diaphragm should provide a temporary bond so that the sensor can be removed from the fixture once the calibration has been completed. The upper fixture adhesive should have the following characteristics:

a) be strong enough to transfer the normal and shear loads across the interface,

b) be weak enough in peel to allow removal from the NSST diaphragm without causing the diaphragm to exceed its elastic limit,

c) be flexible enough to allow the polymer and diaphragm surfaces to deform under load, and

d) be compatible with steel and neoprene.

The double-sided tapes purchased for experimentation are shown in Table 13. The choices for a double-sided tape with a temporary bond are very limited.

Table 13. Double-sided Tapes for NSST Fixture

Brand	Model	Type	Adhesive	Adhesion (oz/in)	Thickness (mils)	Ref.
ECHOtape	DC-K048A	Temporary	Rubber	47	6	[16]
ECHOtape	DC-M012P	Permanent	Acrylic	70	8	[17]
ECHOtape	DC-U032A	Permanent	Acrylic	80	9.5	[18]
3M	9832	Permanent	Acrylic	58	4.8	[19]

3.7 Summary

A NSST calibration rig has been designed around two linear actuators arranged in a YZ orientation and a 3-axis load cell (see Figure 8). The transverse deflection of the Y-actuator and the tip displacements of the Z-Stage support structures under design loads were analyzed. All deflections were within acceptable limits. Material options were found for the Polymer Cylinder and Double-Sided Tape that form part of the NSST fixture. The final selection of these two materials can only be made through experimentation.

4. PROTOTYPE NSST FABRICATION AND INSTRUMENTATION

The validation of the NSST calibration rig design requires a NSST sensor. The validation of a NSST sensor design needs a NSST calibration rig. The validation of one needs the validation of the other. To resolve this dilemma, prototype NSST sensors were fabricated so that the calibration rig design could be validated first. This order of validation is justified because of Micron Instruments' extensive experience with the design and behavior of the NSST sensor's predecessor the Dual Bond Stress and Temperature (DBST) sensor [1]. This Section documents the fabrication of a prototype NSST sensor that is appropriate for the validation of the NSST calibration rig. The sealing technique used in the prototype NSST is not appropriate for installation in a solid rocket motor because the diaphragm cavity is not sealed.

4.1 Prototype NSST Sensor Wiring

Figure 15 shows the gage positions and wiring plan for the prototype NSST. The gages are located at the coordinates specified in [2]. The connector terminal number, signal type, signal label and wire color are shown. Recall that the NSST sensor is designed such that the shear bridge must be aligned in the direction of maximum shear.

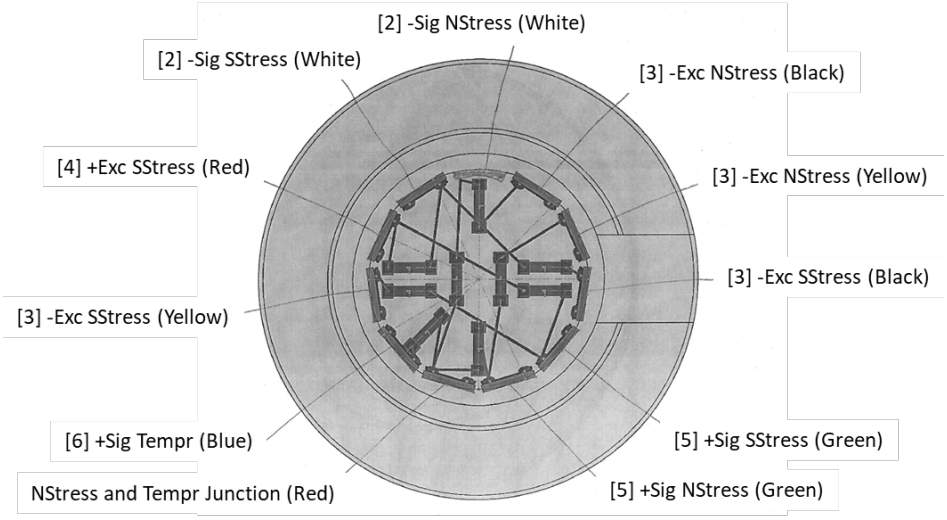

Figure 15: Prototype NSST wiring diagram. NStress = Normal, SStress = Shear.

Figure 16 provides the circuit schematics for the normal stress and temperature bridge and the shear stress bridge. The normal stress and temperature bridge requires completion resistors for the temperature bridge. These completion resistors are contained on an off-board miniature circuit board that is not shown.

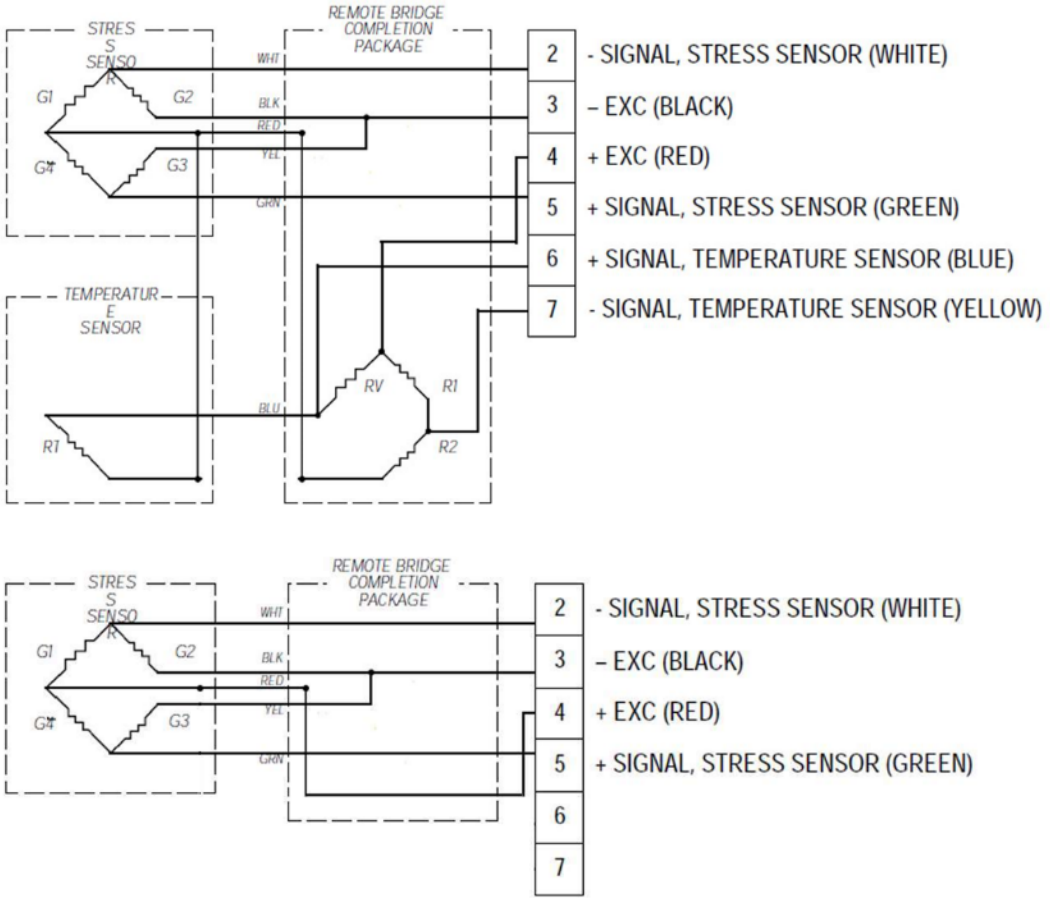

Figure 16: Wheatstone bridge schematics. Top = Normal stress-Temperature bridge, Bottom = Shear stress bridge.

4.2 Prototype NSST Sensor Fabrication

Figure 17 to Figure 19 illustrate the steps to fabricate a prototype NSST. The SS-037-033-500P gages are bonded to the sensor diaphragm (Figure 17). The gage lead wires are soldered to the sidewall tabs along with the magnet wires. The magnet wires are then threaded through the printed circuit board header (Figure 18). Finally, the printed circuit board is bonded to the sensor body and the magnet wires are bundled and bonded to the circuit board and sensor body (Figure 19).

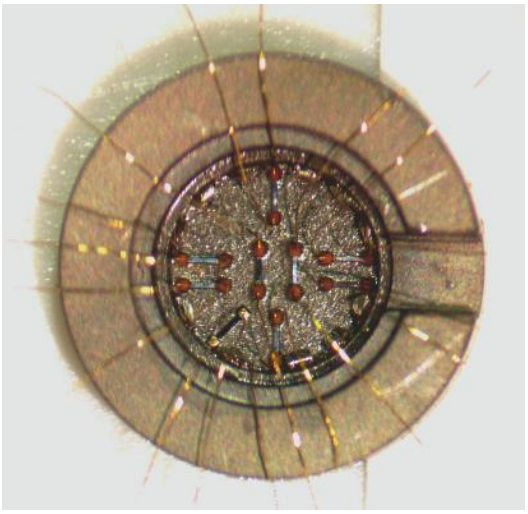

Figure 17: NSST sensor body with bonded Normal stress-Temperature gages and Shear stress gages.

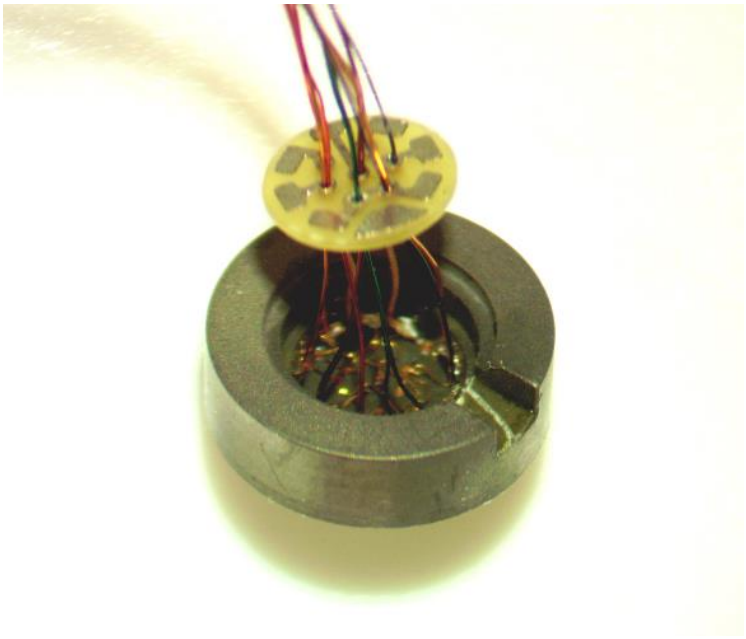

Figure 18: NSST sensor body with soldered gold leads and magnet wire. Magnet wires are threaded through the printed circuit board header.

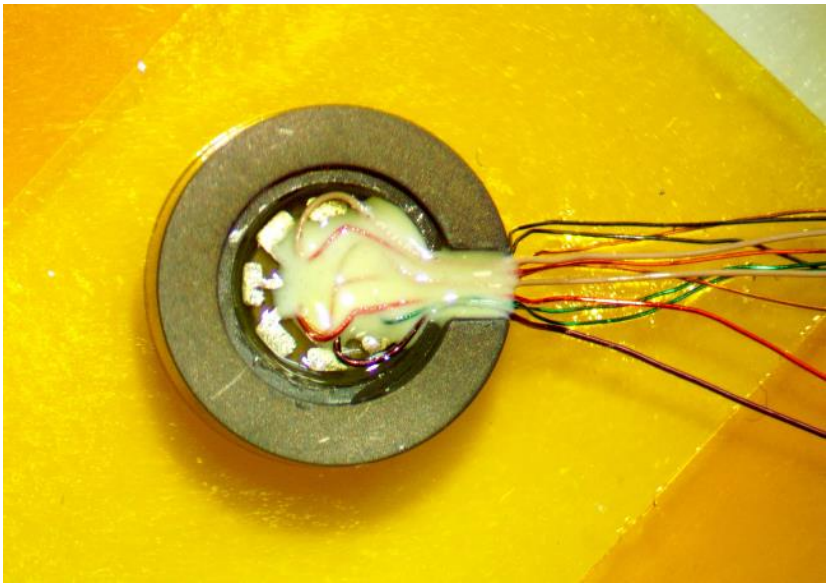

Figure 19: Completed prototype NSST sensor with bonded magnet wires that lead to bridge completion boards (not shown).

A total of four prototype NSST sensors were built. The individual gage resistances are recorded in Table 14.

Table 14. NSST Gage Resistances

	Normal and Temperature Gages					Shear Gages			
NSST	G1 (ohms)	G2 (ohms)	G3 (ohms)	G4 (ohms)	RT (ohms)	G1 (ohms)	G2 (ohms)	G3 (ohms)	G4 (ohms)
1	470	471	471	476	4925	481	479	479	478
2	471	483	477	480	5023	467	477	472	470
3	478	488	480	490	5229	484	480	479	476
4	473	486	479	497	4894	467	471	466	477

4.3 NSST Null Balance

If the gages in Table 14 were connected as shown in Figure 16, the bridge output at zero load would be non-zero because of the resistance differences among the four gage resistances. Also, the bridge output would be very sensitive to any temperature changes the strain gages may experience. To bring the bridge to a near zero output condition at no

load and to have the bridge self-compensate for changes in temperature, the bridge can be nulled and compensated using a set of series and shunt resistors in the bridge circuit.

Figure 20 shows the possible null-balance and temperature compensation resistors which could be added to the basic Wheatstone bridge circuit. The resistors consist of series resistor, RS, and parallel resistor, RP, before the bridge, the RZ1 and RZ4 shunt resistors acting on gages G1 and G4, respectively, and RB2 and RB3 series resistors acting on the left and right branches, respectively, in the bridge. Only one shunt resistor, RZ1 or RZ4, is needed and only one series resistor, RB2 or RB3, is needed.

To wire up the bridge, RED is attached to the positive excitation, YEL and BLK are attached to the negative excitation, GRN is attached to the positive signal line and WHT is attached to the negative signal line.

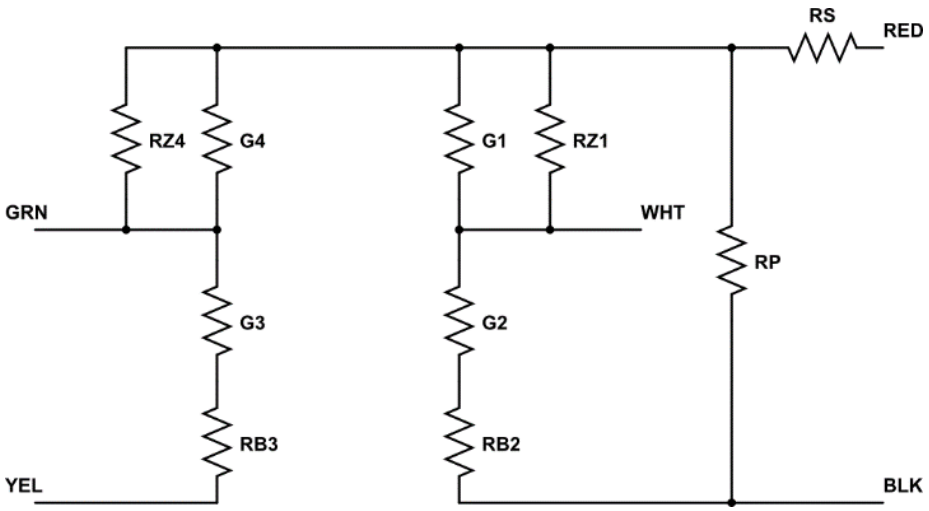

Figure 20: Compensation resistors to achieve null bridge output at zero load and compensation for temperature changes.

It has been found that the temperature coefficient of resistance of Micron gages are quite well matched. This matching means that the gages change resistance with temperature at the same rate. So, in general, no shunt resistor, RZ1 or RZ4, is needed.

Also, it has been found that a RS equal to 3000 ohms and a RP equal to 3000 ohms allow a good degree of temperature compensation to be obtained. The null condition can be achieved by selecting the proper series resistor RB2 or RB3. It should be noted that these values of RS, RP, RZ1, RZ4 and RB2 or RB3 will not scale the bridge output to a desired value. For the purposes of preliminary testing, a null bridge balance with temperature insensitivity is sufficient for this work.

The value of RB2 or RB3 can be calculated using the following equations,

$$\textit{assuming RB2 = 0,} \quad RB3 = \frac{RG2 \cdot RG4 - RG1 \cdot RG3}{RG1} \tag{2}$$

$$\textit{assuming RB3 = 0,} \quad RB2 = \frac{-RG2 \cdot RG4 + RG1 \cdot RG3}{RG4} \tag{3}$$

where *RBn* and *RGn* are resistance values of the series resistor and gage resistance, respectively. The proper series resistor, RB2 or RB3, will be indicated by a positive value for either equation 2 or 3.

The calculated RB resistors for the four prototype NSST sensors are shown in Table 15. The temperature bridge circuit was completed using default resistors for R1, R2 and RV (see Figure 15). No attempt was made to scale its output since it is not of interest here.

Table 15. NSST Null Balance Resistors

	Normal		Shear	
NSST	RB	Value (ohms)	RB	Value (ohms)
1	3	5.62	2	2.26
2	3	15	3	7.32
3	3	20	2	6.65
4	3	30	3	15

4.4 NSST Instrumentation

The NSST requires two constant current 4 mA power supplies and two multimeters to function. Two Keithley 2450 source meter units are used as power sources in the experimental set-up [21]. One Keithley DAQ6510 is programmed to read the two bridge outputs [22].

As discussed in Sub-Section 3.2, linear actuators are employed to manually apply normal and shear displacements to the NSST fixture. The resultant forces are measured by an Interface 3A120 200N 3-axis load cell (see Figure 8) [6]. The electrical signals from the loadcell are digitized by an Interface BSC4D amplifier [23] and read by their BlueDAQ application which runs on a laptop computer. The load cell/amplifier combination was calibrated at the factory before being shipped.

5. CALIBRATION RIG AND NSST PRELIMINARY MEASUREMENTS

Before attempting the calibration of a NSST sensor, it is important to examine the nature of the data coming from the NSST sensor and calibration rig in a systematic fashion. There are four studies of interest:

1. Linearity response to applied normal force.
2. Linearity response to applied shear force.
3. Shear bridge insensitivity to NSST sensor angular orientation.
4. Linearity response to applied air pressure.

The baseline NSST fixture configuration consists of neoprene cylinder N70-1 (Table 12), double-sided tape ECHOtape DC-U032A (Table 13) for the neoprene cylinder/lower fixture interface and double-sided tape 3M 9832 (Table 13) for the neoprene cylinder/upper fixture interface and NSST-3. The N70 polymer was selected because it has a modulus that is close to the modulus used in the finite element analyses.

It should be mentioned that many experimental trials (not reported) were carried out beforehand to look at the performance of the double-sided tapes under various magnitudes of loads before settling on the baseline configuration.

The following sub-sections present the results of the studies.

5.1 Linearity Response to Applied Normal Force

The linearity response to applied normal force is shown graphically in Figure 21 to Figure 23. A normal compressive force was applied in increments of 20 N up to 100 N and then stepped down in 20 N increments back to zero load. Compression was used to keep the back of the sensor fully supported against the anvil. The applied maximum normal force is 65% of the calibration rig design load.

Figure 21 shows the NSST normal and shear bridge outputs versus data point number. The applied compressive force is shown for reference. The applied force is not smooth because the compressive displacement is manually applied. The strong viscoelastic effects from the neoprene cylinder complicated the application of a constant force at each load increment.

The maximum normal bridge output is roughly 39 mV for a 100 N normal load. The shear bridge output is roughly 1 mV for a 100 N normal load. Figure 22 plots the ratio of shear bridge output to normal bridge output for the captured data series. The shear to normal crosstalk is 0.033 +/- 0.001 or 3.3 +/- 0.1%.

The normal force calibration factor is shown graphically in Figure 23. The calibration factor is calculated by dividing the measured normal bridge output by the applied normal force at each data point. The normal bridge calibration is 0.39 +/- 0.01 mV per N between data points 102 and 252 or 1.18 +/- 0.03 mV per psi for the neoprene cylinder that was used.

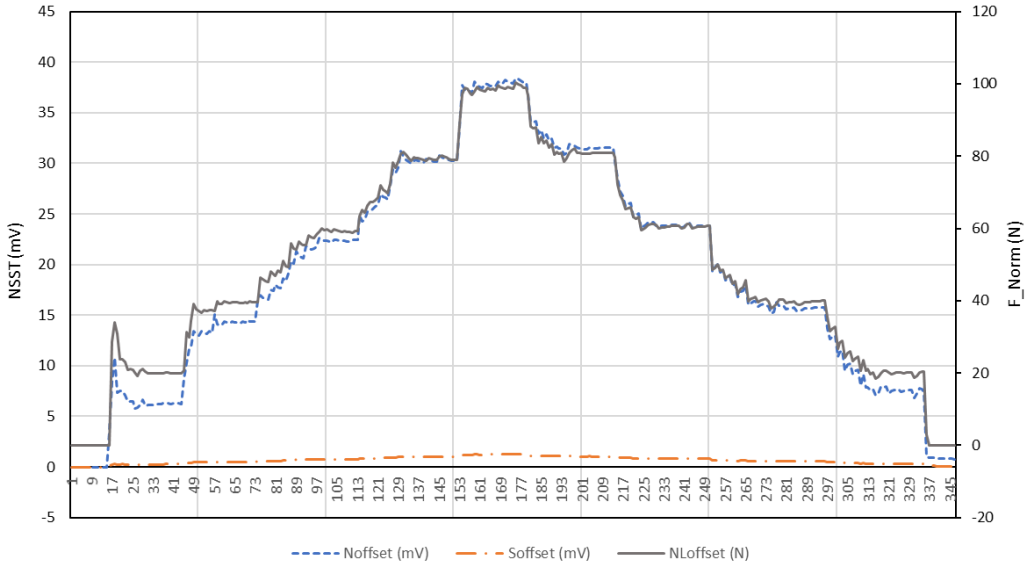

Figure 21: Linearity of NSST response to normal compressive force. Noffset is normal output. Soffset is shear output. NLoffset is applied normal force.

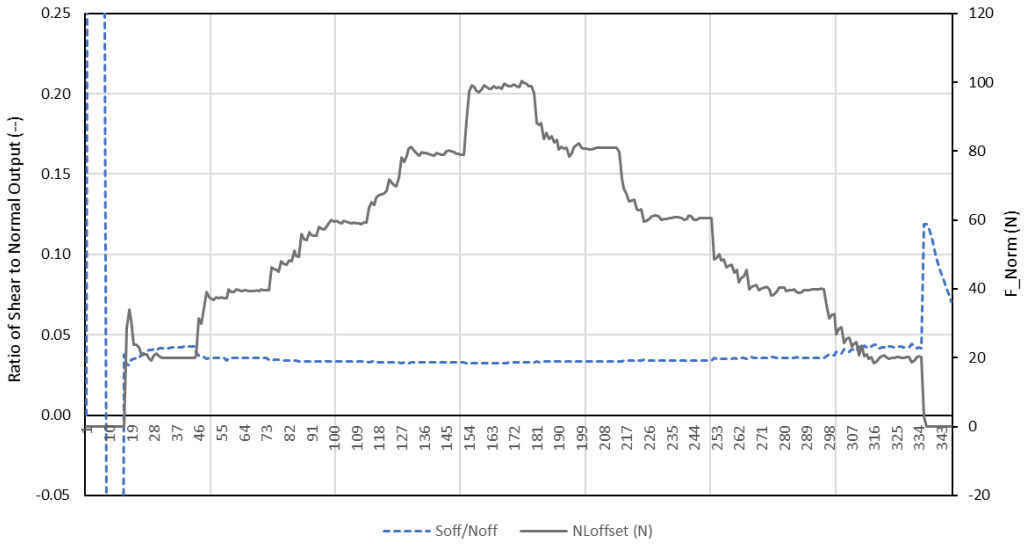

Figure 22: NSST shear to normal bridge crosstalk for a normal compressive force. Soff/Noff is ratio of shear to normal output. NLoffset is applied normal force.

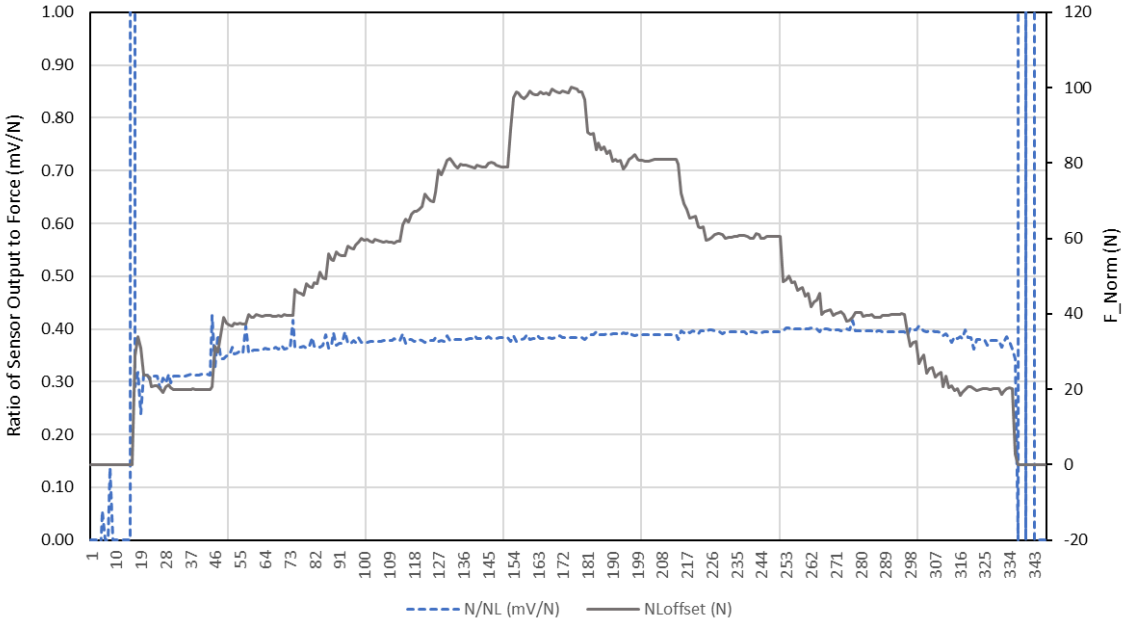

Figure 23: NSST normal force calibration. N/NL is ratio of normal bridge output to applied load. NLoffset is applied normal force.

5.2 Linearity Response to Applied Shear Force

The linearity response to applied shear force is shown graphically in Figure 24 to Figure 26. The shear force was applied in increments of 2 N up to 8 N and then stepped down in 2 N increments back to zero load. The maximum shear force is limited by the shear strength of the 3M 9832 tape. The 8 N force represents 5% of the calibration rig design load.

Figure 24 shows the NSST normal and shear bridge outputs versus data point number. The applied shear force is shown for reference. The applied force is not smooth because the shear displacement is manually applied. The shear bridge and normal bridge outputs are generally linear up to the maximum shear force. The two bridge outputs appear to have a different behavior on the way back to zero load. This behavior was caused by slippage at the upper fixture/neoprene cylinder interface. The shear strength of the 3M 9832 tape was being exceeded.

The maximum shear bridge output is roughly 1 mV for an 8 N shear load. The normal bridge output is roughly 0.8 mV for the 8 N shear load. Figure 25 plots the ratio of the normal bridge output to shear bridge output for the captured data series. The normal to shear crosstalk is roughly 0.25 to 0.80 or 25% to 80% up to the maximum shear load.

The shear force calibration factor is shown graphically in Figure 26. The calibration factor is calculated by dividing the measured shear bridge output by the applied shear force at each data point. The shear bridge calibration is 0.10 +/- 0.01 mV per N between data points 97 and 236 or 0.30 +/- 0.03 mV per psi for the neoprene cylinder that was used.

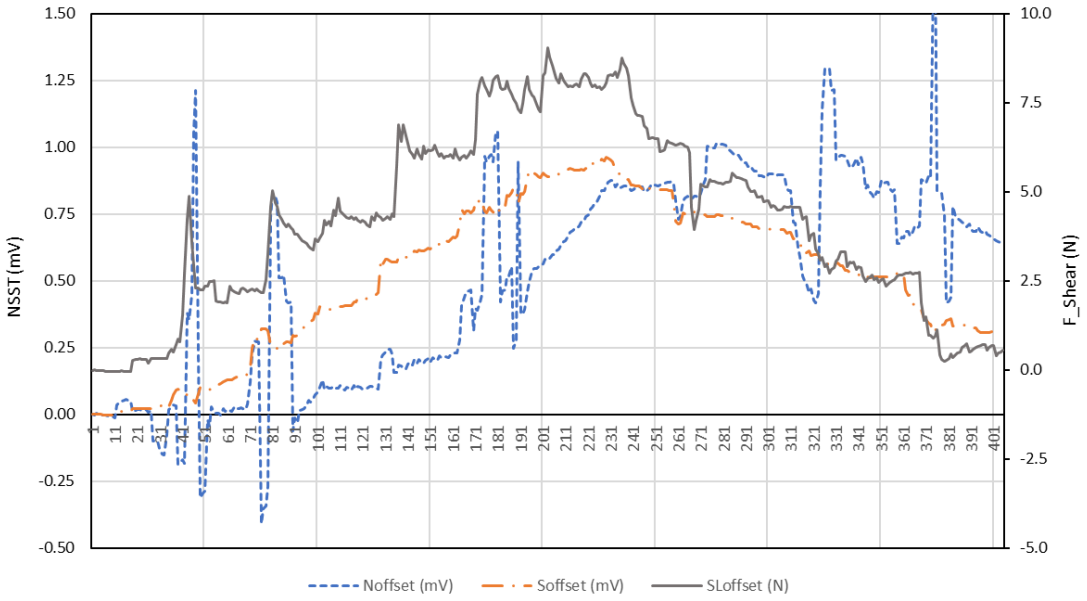

Figure 24: Linearity of NSST response to shear force. Noffset is normal output. Soffset is shear output. SLoffset is applied shear force.

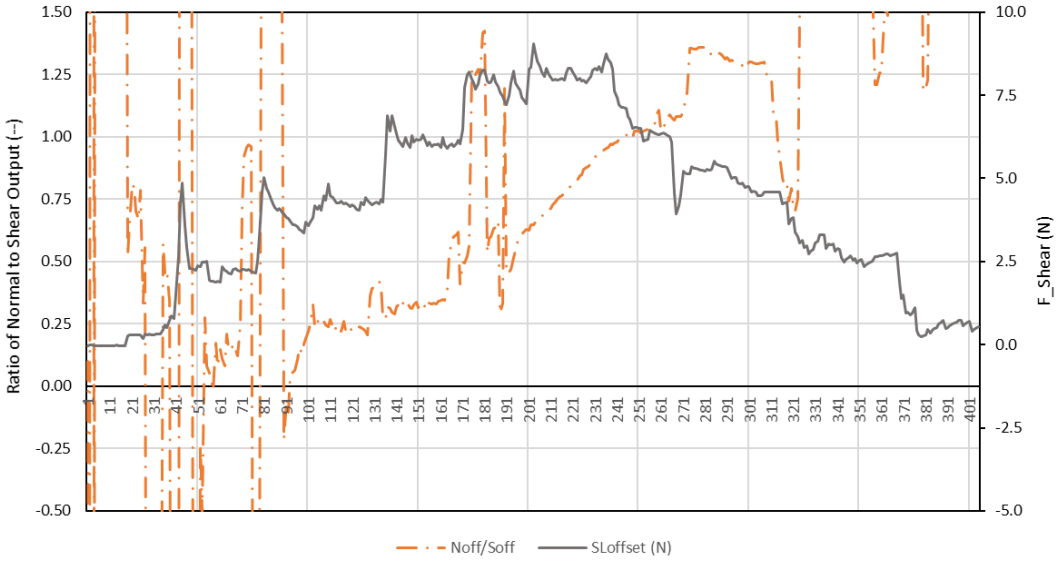

Figure 25: NSST normal to shear bridge crosstalk for a shear force. Noff/Soff is ratio of normal to shear output. SLoffset is applied shear force.

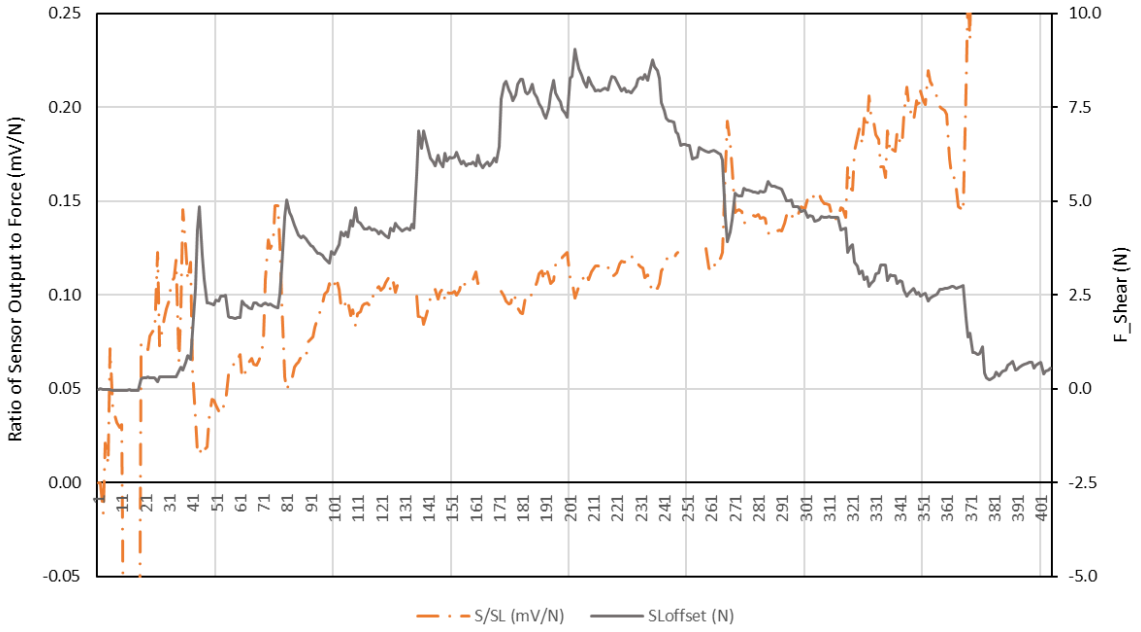

Figure 26: NSST shear force calibration. S/SL is ratio of shear bridge output to applied shear load. SLoffset is applied shear force.

5.3 Shear Bridge Insensitivity

The shear stress bridge, if oriented accurately in a direction perpendicular to the normal stress bridge, should produce a null output if a shear force is applied along the major axis of the normal stress bridge. The output of the normal bridge should be unaffected. For this test, the NSST sensor was rotated 90 degrees in the calibration rig and then the shear force was applied.

Figure 27 shows the shear bridge response to an applied shear force between 0 and 8 N. The shear bridge output is 0.02 +/- 0.01 mV between data points 51 and 148. This output is roughly 2% of the output measured in Sub-Section 5.2 where the shear bridge was oriented along the major shear axis.

In contrast, when a normal force is applied to the sensor (see Figure 28 and Figure 29), a normal bridge calibration of 0.39 +/- 0.01 mV per N between data points 52 and 159 is measured along with a shear to normal output crosstalk of 0.037 +/- 0.001 mV. These values compare favorably to the calibration and crosstalk values measured in Sub-Section 5.1 where the normal bridge was oriented in a perpendicular direction to the major shear axis.

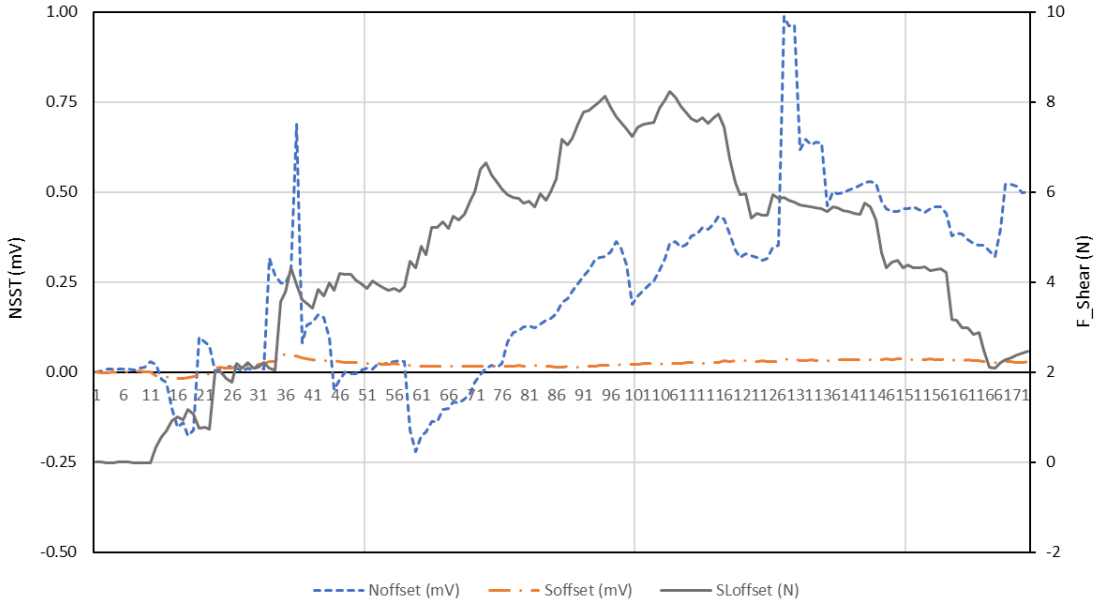

Figure 27: Responses of bridges where normal bridge is oriented inline with major shear axis.

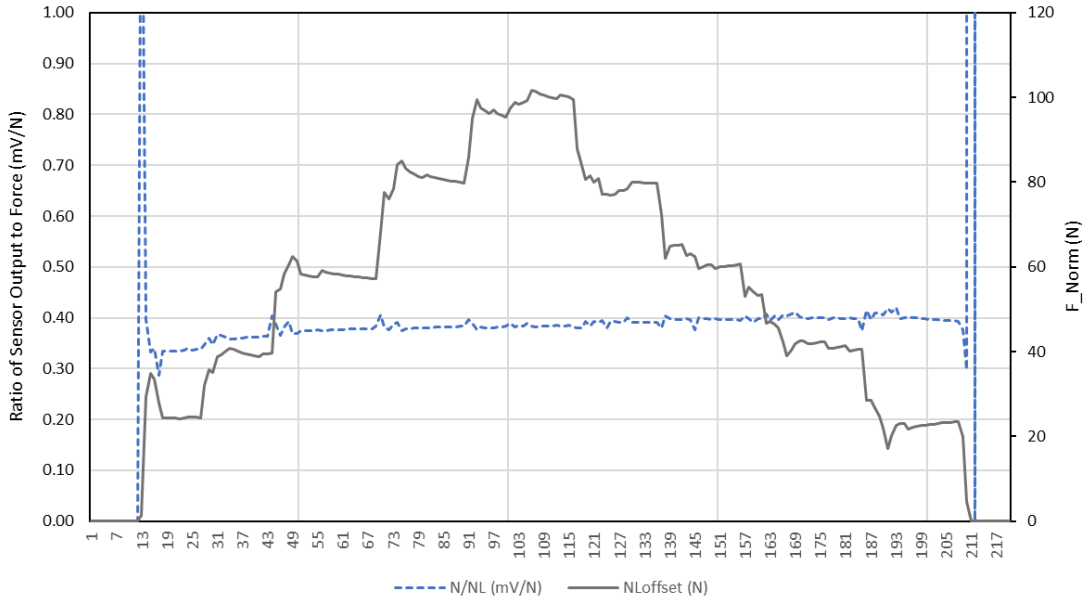

Figure 28: Response of normal bridge that is oriented inline with major shear axis. N/NL is the calibration factor.

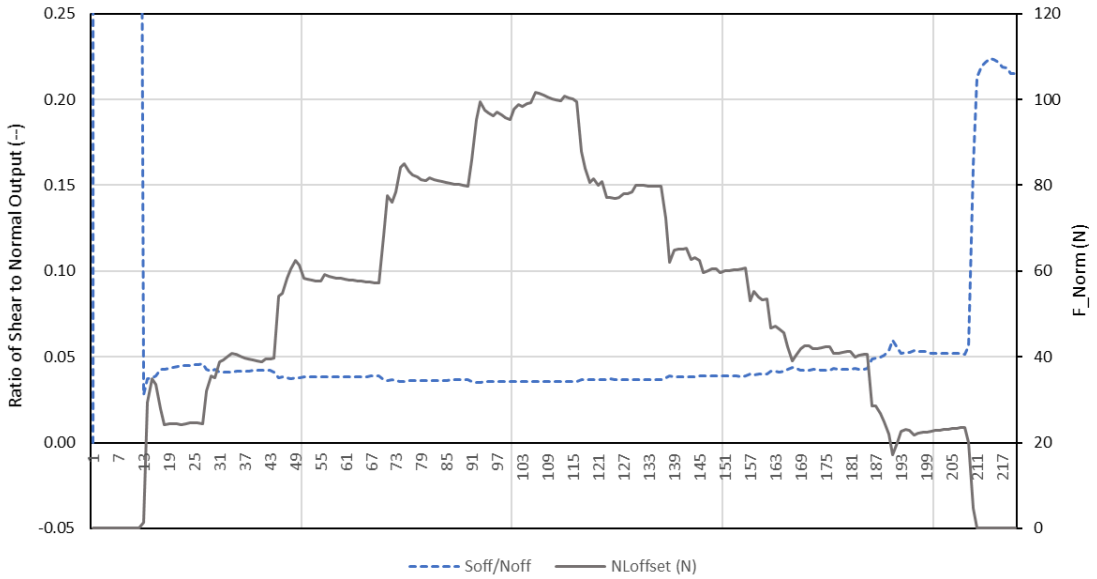

Figure 29: NSST shear to normal bridge crosstalk where normal bridge is oriented inline with major shear axis. Soffset/Noff is shear to normal output ratio.

5.4 Linearity Response to Applied Air Pressure

To validate that the stress loading through the polymer cylinder is equivalent to a traction-free air pressure loading, the NSST sensor was installed in a gas manifold and pressurized up to 50 psi in increments of 10 psi with a regulator and compressed air source.

Figure 30 plots the shear to normal output crosstalk. The crosstalk ratio is 0.041 +/- 0.002. This value is 24% higher than the crosstalk seen for loading through a polymer cylinder (0.033 +/- 0.001 from Sub-Section 5.1).

The calibration factor result is shown in Figure 31. For an air pressure loading, the calibration factor is 1.09 +/- 0.02 mV/psi. This value is 7% lower than the calibration factor seen for loading through a polymer cylinder (1.18 +/- 0.03 mV per psi from Sub-Section 5.1).

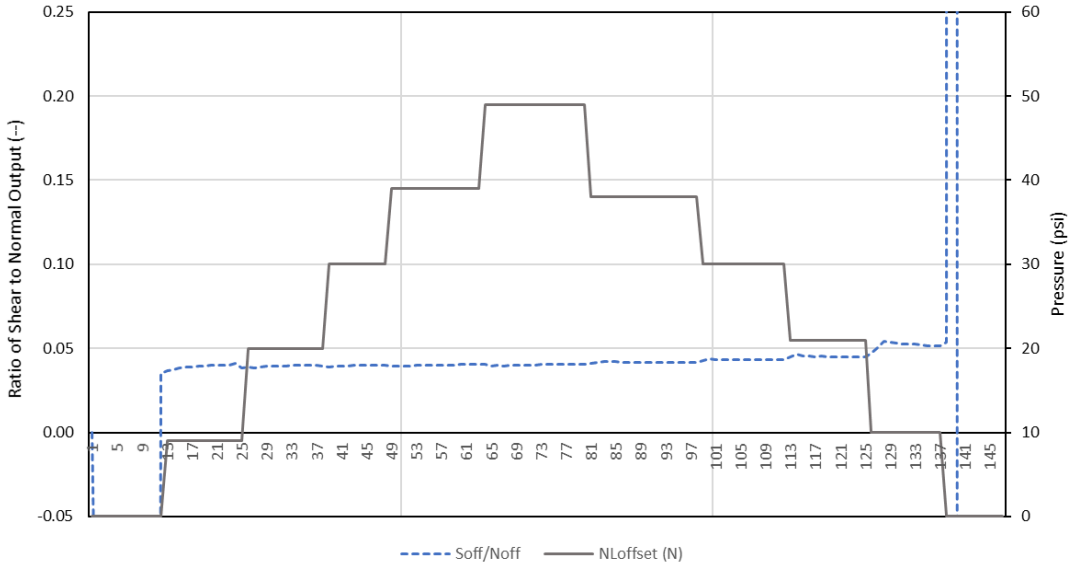

Figure 30: NSST shear to normal bridge crosstalk for compressive air pressure. Soff/Noff is shear to normal output ratio.

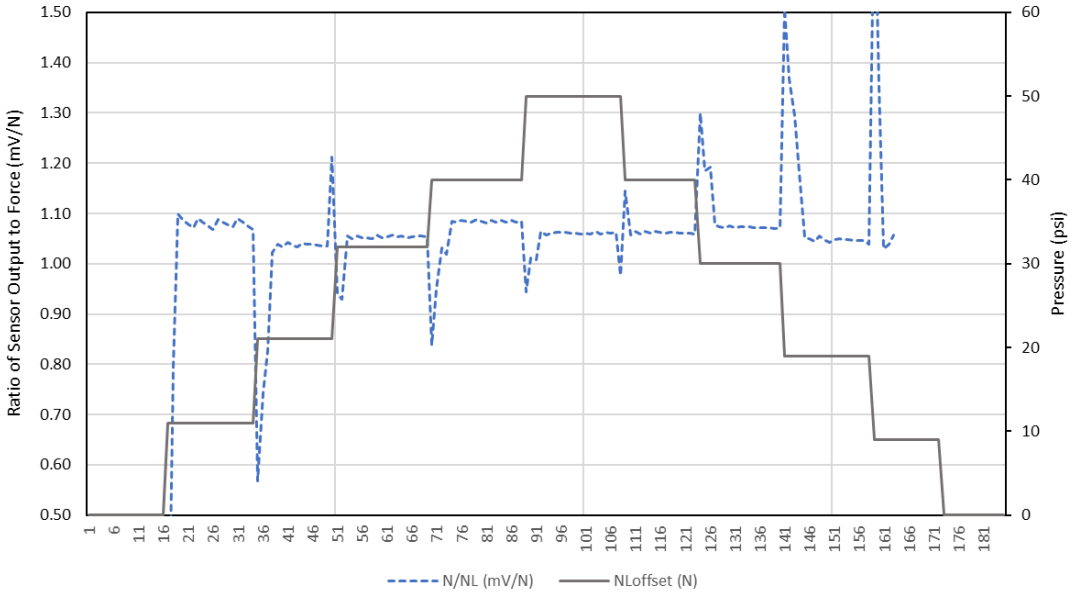

Figure 31: NSST normal pressure calibration. N/NL is ratio of normal bridge output to applied pressure. NLoffset is applied pressure.

5.5 Discussion

The preliminary tests show that the NSST calibration rig can apply the desired normal and shear forces. The instrumentation set-up allows simultaneous measurement of the NSST output signals and the applied force components. Controlling the applied forces requires an operator to become familiar with the viscoelastic nature of the neoprene cylinder and to practice applying Y and Z displacements to compensate for the time-varying forces. The quality of the calibration, at this point, depends on the ability of the operator to monitor the instantaneous force components and their rates of change to turn the two actuator wheels in the proper direction to counter the rates of change.

The response of the NSST sensor to normal force is adequate in the sense that the normal bridge outputs a large signal in relation to the applied force while the shear bridge outputs a much smaller signal. The low crosstalk makes distinguishing normal forces from shear forces straightforward. A normal bridge calibration factor of 0.39 +/- 0.01 mV/N was determined.

The response of the NSST to shear force is less clear. The output of the shear bridge was on the same order of magnitude as the normal bridge for the maximum shear force that the upper fixture 3M double-sided tape could support. A shear calibration factor of 0.11 +/- 0.01 mV/N was determined.

Even though the crosstalk for the shear bridge is large, there should be no confusion whether the shear bridge output is being caused by a shear force or a normal force because the normal bridge will output a large signal if a normal force is actually being applied.

The lack of a measured response from the shear bridge oriented in a direction perpendicular to the applied shear force occurred as expected. The location of the shear bridge along the null line of the asymmetric deformation of the diaphragm (see [2]) meant that it would not see any of the shearing strains along the shear bridge's major axis.

Both the crosstalk and calibration factor measured by air pressure loading are reasonably close to their respective values measured by loading through a polymer cylinder. The 24% higher crosstalk seen for the air loading suggests a degree of reinforcement from the polymer cylinder that reduces the degree of strain seen by the shear bridge is possible. The 7% lower calibration factor seen in the air loading suggests a less efficient transfer of load into the diaphragm.

The experimentally measured normal to shear output ratio is 3.9 +/- 0.5 (0.39 +/- 0.01 mV/N divided by 0.10 +/- 0.01 mV/N). This value compares favorably to the predicted normal to shear output ratio from the finite element analysis. Figure 1 shows that an 880 micron normal bridge output (ε_tens) was predicted for a 50 psi normal stress while a 220 micron shear bridge output (ε_shear) was predicted for a 50 psi shear stress. These

predictions give a predicted normal to shear output ratio of 4 (880 micron/50 psi divided by 220 micron per 50 psi). These values are summarized in Table 16.

Table 16. Predicted and Measured NSST Parameters

	Predicted	**Measured**
Normal strain, ε_tens	880 ε/50 psi	0.39 +/- 0.01 mV/N
Shear strain, ε_shear	220 ε/50 psi	0.10 +/- 0.01 mV/N
Ratio, ε_tens/ε_shear	4	3.9 +/- 0.5

The comparable predicted and experimental normal to shear output ratios give assurance that the finite element techniques used to model the NSST sensor, its diaphragm, the supporting structures surrounding the NSST sensor and the far field loading conditions are valid. Furthermore, since the calibration conditions are correctly modeled, it stands to reason that the predictions in [2] for the response of a NSST sensor installed in a motor bondline would also be reasonable.

6. NSST CALIBRATION

Four prototype NSST sensors were fabricated (see Section 4). NSST-4 was used in many of the undocumented tests to evaluate sensitivity of normal and shear loads to Y and Z displacements, shear limits of the double-sided tape and methods to mount and unmount the NSST sensor from the double-sided tape and upper fixture. The magnetic wires were subjected to many bending and stretching cycles and eventually broke. Consequently, only the calibration results for NSST-1, NSST-2 and NSST-3 are available.

NSST-1, NSST-2 and NSST-3 were calibrated using a two-point step load from 0 to 100 N for the normal load and 0 to 8 N for the shear load. This method of calibration gave more consistent results. Figure 32 shows the NSST calibration rig set-up.

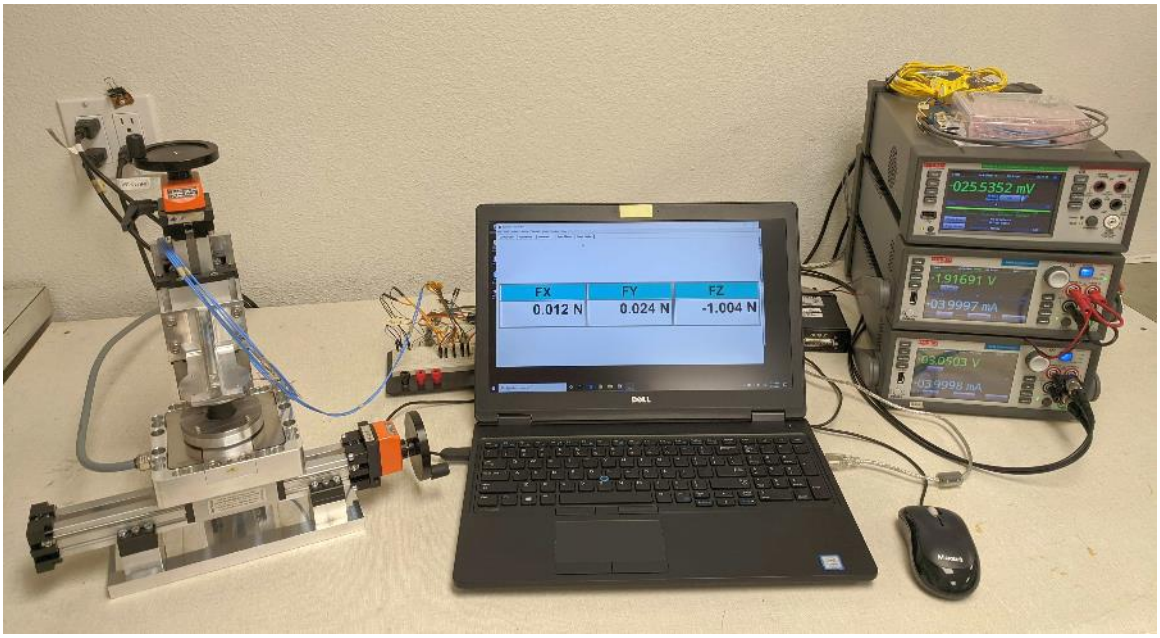

Figure 32: NSST calibration rig with the 3-axis loadcell data acquisition system and the Keithley 6510 meter and two 2450 power sources.

6.1 Calibration of NSST-1

The normal force calibration factor and shear to normal output crosstalk is shown graphically in Figure 33 and Figure 34, respectively. The normal bridge calibration was evaluated to be 0.43 +/- 0.01 mV per N between data points 20 and 77 or 0.19 +/- 0.004 mV per kPa or 1.30 +/- 0.03 mV per psi. The shear to normal crosstalk was evaluated at 0.10 +/- 0.001 mV per mV between the same data points. The shear force calibration factor is shown in Figure 35. The shear bridge calibration was evaluated to be 0.13 +/-

0.01 mV per N between data points 25 and 80 or 0.06 +/- 0.004 mV per kPa or 0.39 +/- 0.03 mV per psi.

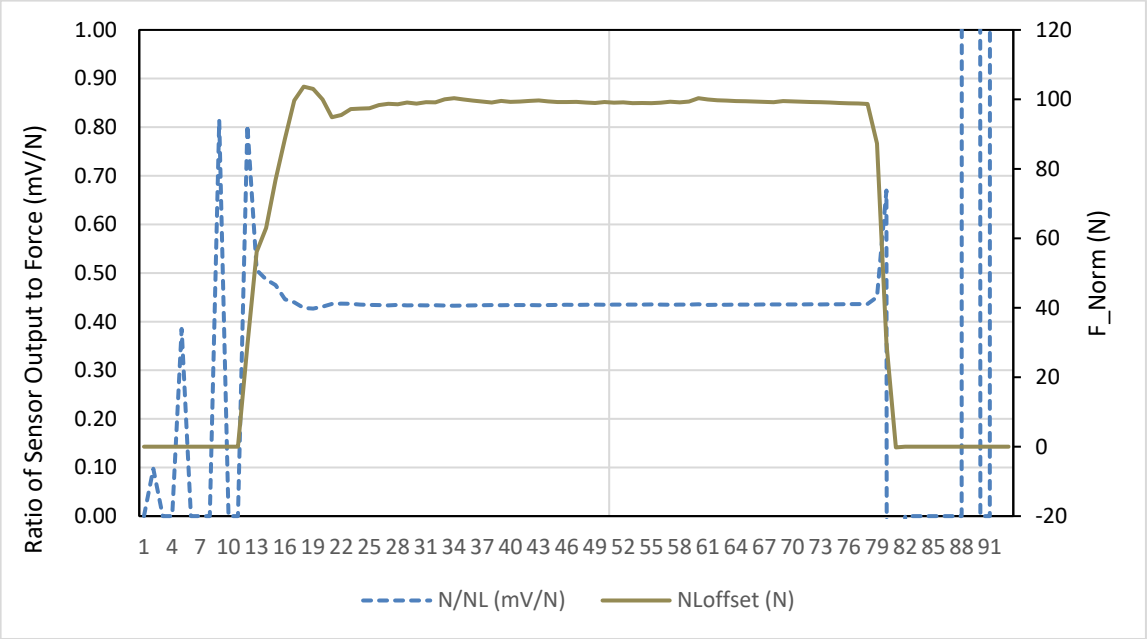

Figure 33: NSST-1 normal force calibration. N/NL is ratio of normal bridge output to applied load. NLoffset is applied normal force.

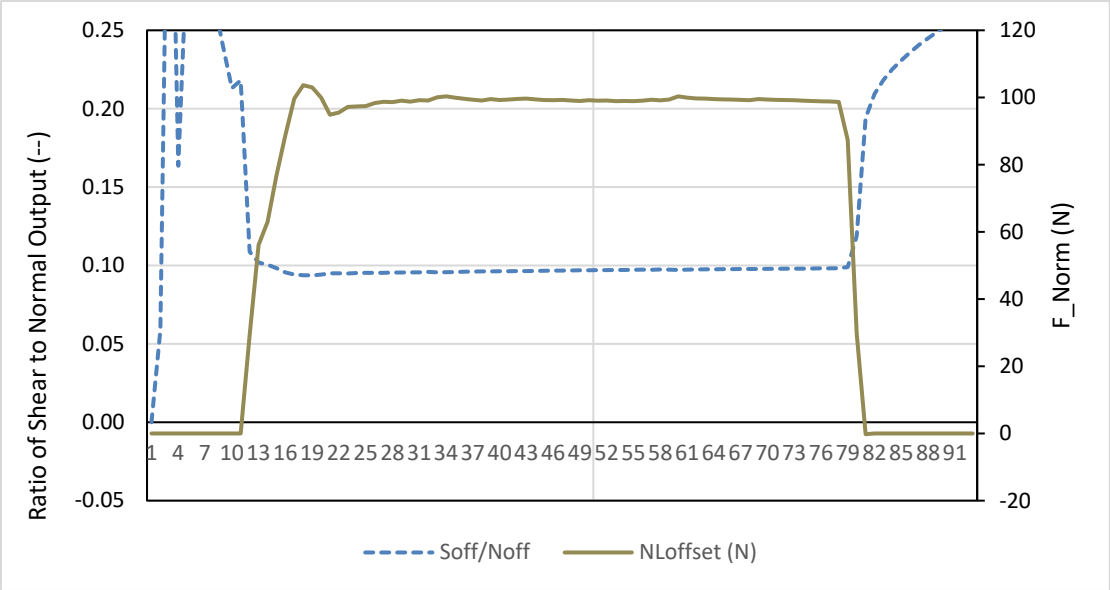

Figure 34: NSST-1 shear to normal bridge crosstalk for a normal compressive force. Soff/Noff is ratio of shear to normal output. NLoffset is applied normal force.

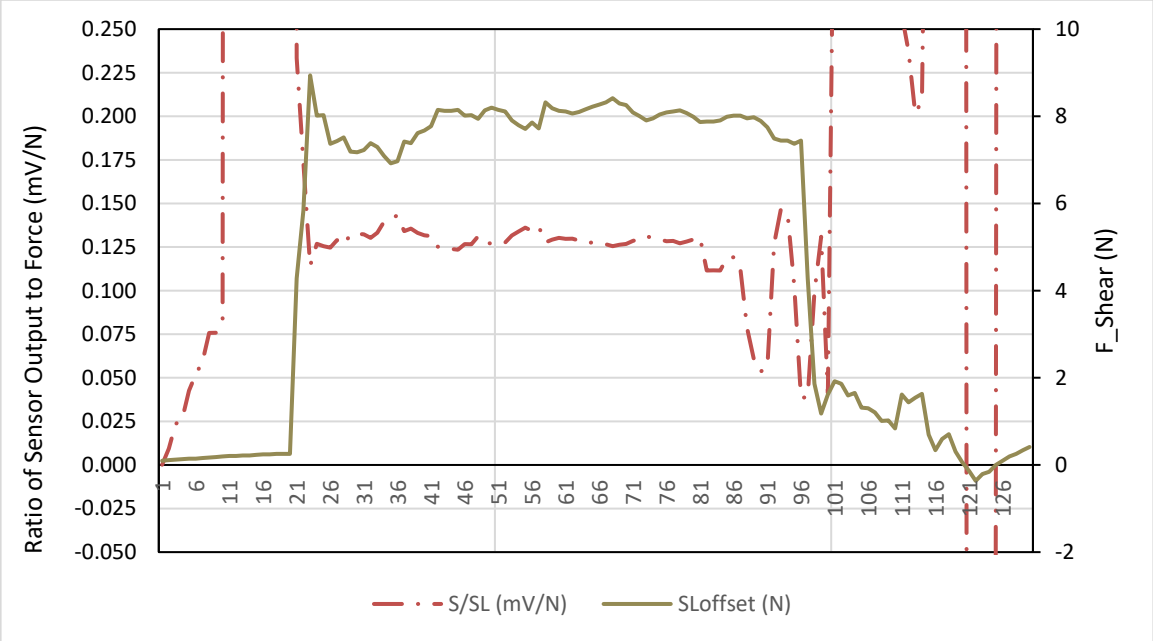

Figure 35: NSST-1 shear force calibration. S/SL is ratio of shear bridge output to applied shear load. SLoffset is applied shear force.

6.2 Calibration of NSST-2

The normal force calibration factor and shear to normal output crosstalk is shown graphically in Figure 36 and Figure 37, respectively. The normal bridge calibration was evaluated to be 0.37 +/- 0.01 mV per N between data points 25 and 88 or 0.16 +/- 0.004 mV per kPa or 1.12 +/- 0.03 mV per psi. The shear to normal crosstalk was evaluated at 0.044 +/- 0.002 mV per mV between the same data points. The shear force calibration factor is shown in Figure 38. The shear bridge calibration was evaluated to be 0.11 +/- 0.01 mV per N between data points 36 and 88 or 0.05 +/- 0.004 mV per kPa or 0.33 +/- 0.03 mV per psi.

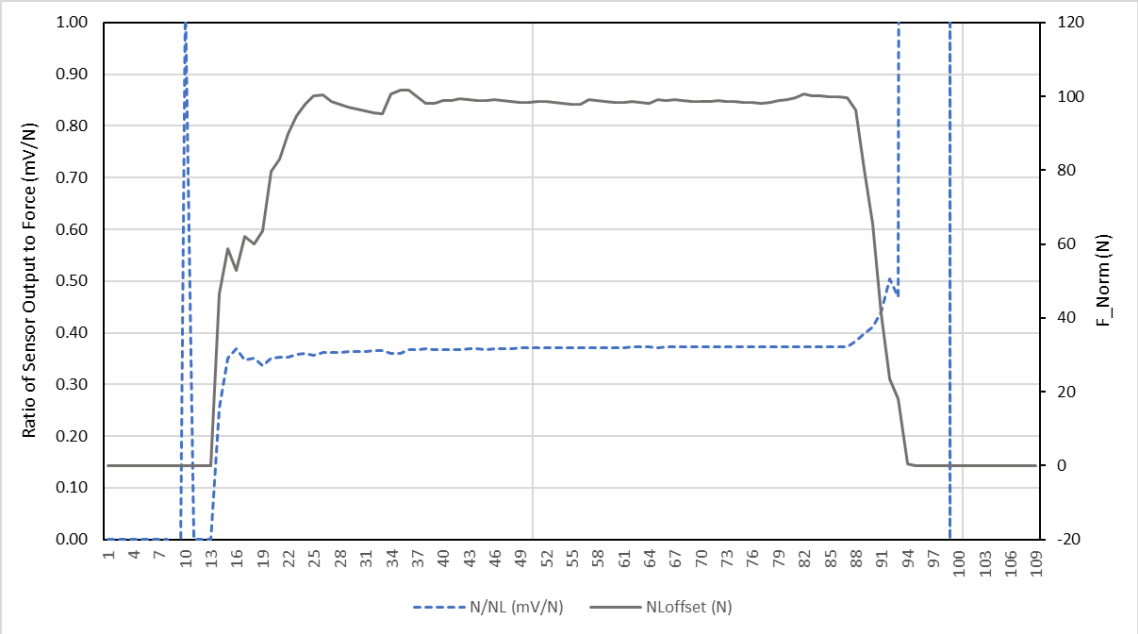

Figure 36: NSST-2 normal force calibration. N/NL is ratio of normal bridge output to applied load. NLoffset is applied normal force.

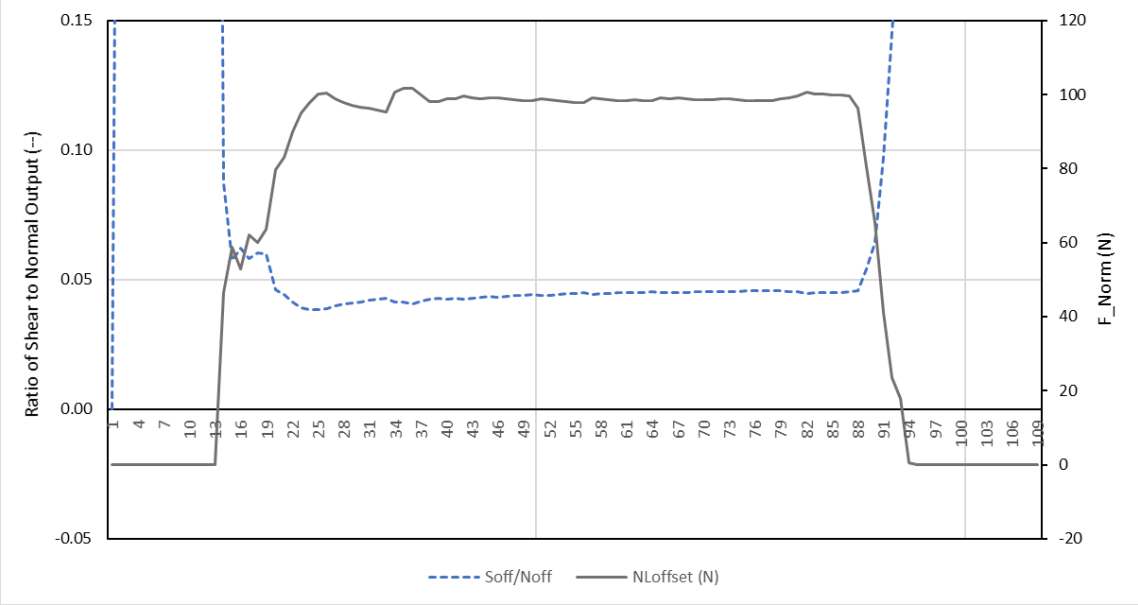

Figure 37: NSST-2 shear to normal bridge crosstalk for a normal compressive force. Soff/Noff is ratio of shear to normal output. NLoffset is applied normal force.

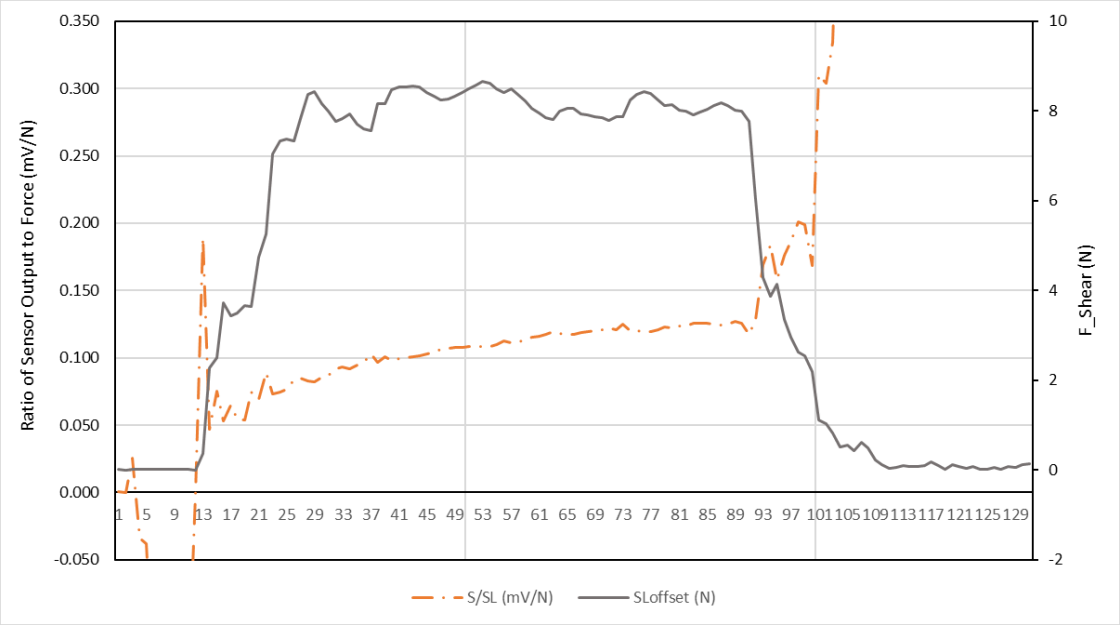

Figure 38: NSST-2 shear force calibration. S/SL is ratio of shear bridge output to applied shear load. SLoffset is applied shear force.

6.3 Calibration of NSST-3

The normal force calibration factor and shear to normal output crosstalk is shown graphically in Figure 39 and Figure 40, respectively. The normal bridge calibration was evaluated to be 0.40 +/- 0.01 mV per N between data points 27 and 89 or 0.18 +/- 0.004 mV per kPa or 1.21 +/- 0.03 mV per psi. The shear to normal crosstalk was evaluated at 0.033 +/- 0.001 mV per mV between the same data points. The shear force calibration factor is shown in Figure 41. The shear bridge calibration was evaluated to be 0.11 +/- 0.01 mV per N between data points 48 and 121 or 0.05 +/- 0.004 mV per kPa or 0.33 +/- 0.03 mV per psi.

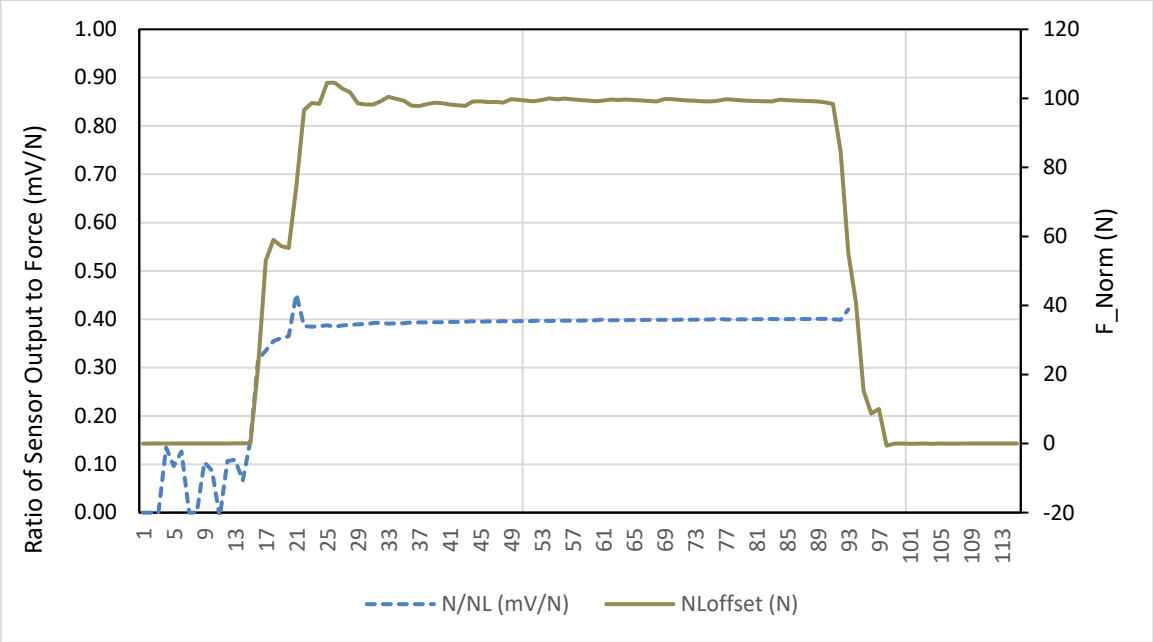

Figure 39: NSST-3 normal force calibration. N/NL is ratio of normal bridge output to applied load. NLoffset is applied normal force.

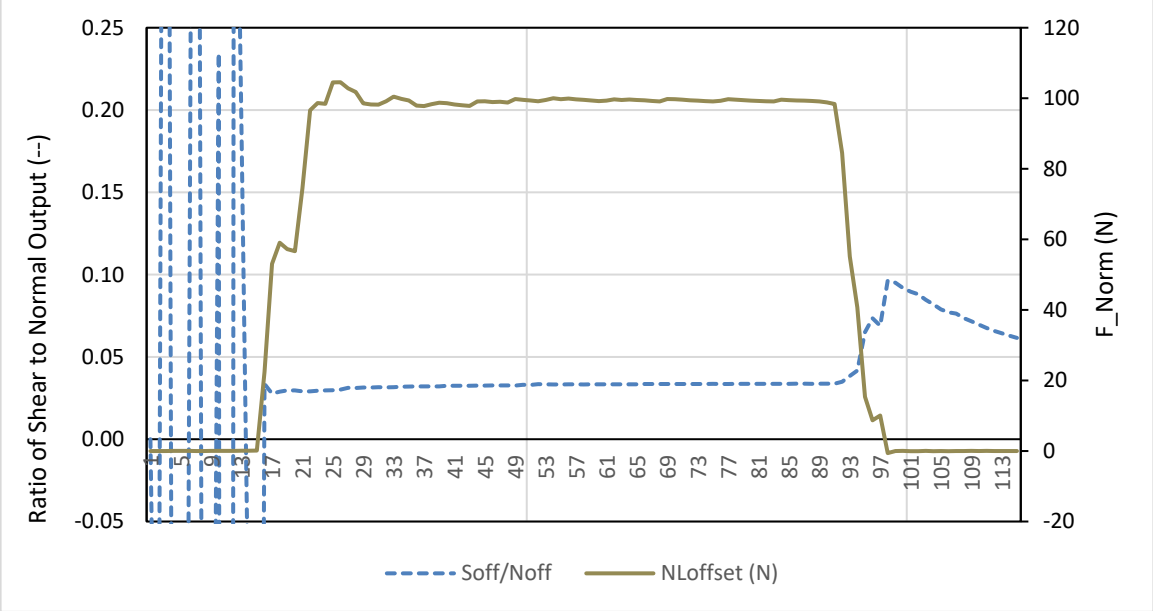

Figure 40: NSST-3 shear to normal bridge crosstalk for a normal compressive force. Soff/Noff is ratio of shear to normal output. NLoffset is applied normal force.

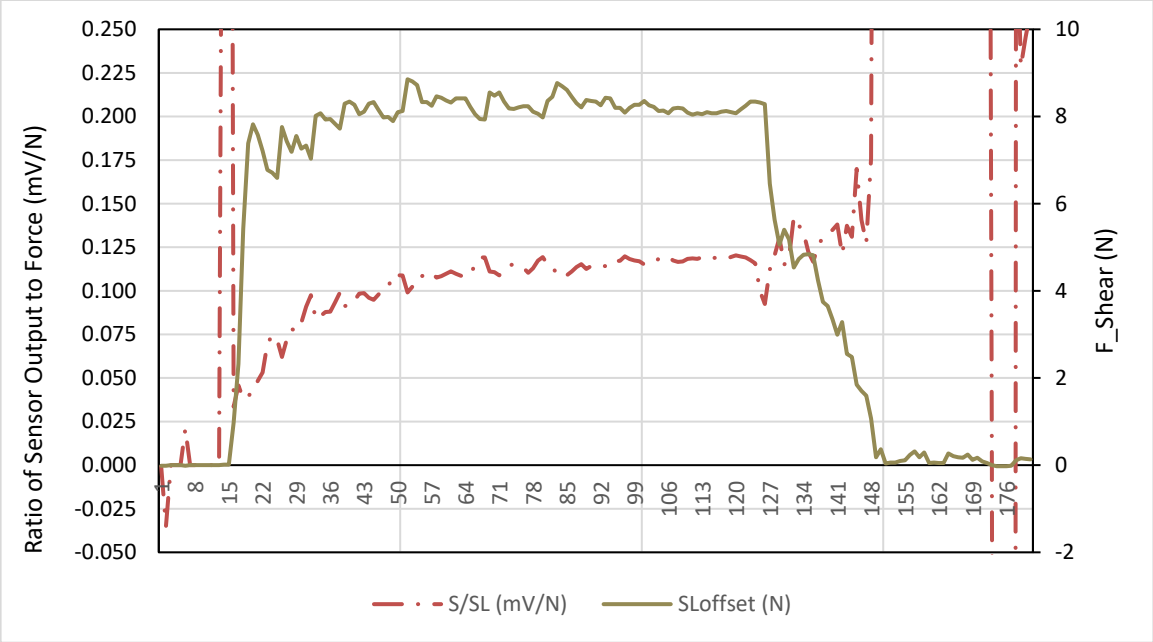

Figure 41: NSST-3 shear force calibration. S/SL is ratio of shear bridge output to applied shear load. SLoffset is applied shear force.

6.4 Discussion

Table 17 summarizes the normal and shear calibration factors measured in this Section. The calibration factors have been listed in terms of mV per N for convenience. The normal calibration factors vary from 0.37 to 0.43 mV per N. The shear calibration factors vary from 0.10 to 0.13 mV per N. The calibration factors for NSST-3 are repeated from Section 5. The multistep load application used in Section 5 and the single step load application used in this Section yielded essentially the same results. The ratio of normal to shear outputs varied between 3.4 +/- 0.4 and 3.9 +/- 0.5. These ratios are reasonably close to the theoretical ratio of 4 from the finite element analysis.

Table 17. Summary of NSST Sensor Calibration Factors

	Normal Calibration (mV per N)	**Shear Calibration (mV per N)**	**Ratio Normal to Shear Calibration**
NSST-1	0.43 +/- 0.01	0.13 +/- 0.01	3.4 +/- 0.4
NSST-2	0.37 +/- 0.01	0.11 +/- 0.01	3.4 +/- 0.4
NSST-3	0.40 +/- 0.01	0.11 +/- 0.01	3.7 +/- 0.4
NSST-3 (Sec. 5)	0.39 +/- 0.01	0.10 +/- 0.01	3.9 +/- 0.5

7. SUMMARY

The objective of this study was to design a calibration rig for a diaphragm-based normal shear stress and temperature (NSST) sensor. The design of a 'milling machine' type NSST calibration rig was presented. Preliminary tests evaluating the ability of the calibration rig to apply pure normal and pure shear to the NSST sensor showed that the calibration rig applied the loading boundary conditions to the NSST sensor in a manner that was consistent with the boundary conditions used in the NSST finite element analysis. The application of load through a polymer cylinder was comparable to application of load through compressed air thereby validating the use of a polymer cylinder to transmit load from the calibration rig to the sensor diaphragm.

The experimentally measured NSST ratio of normal to shear bridge output matched reasonably well the predicted finite element NSST ratio of normal to shear bridge output. This result gives confidence that the modeling technique employed in [2] is valid and that the predictions made in [2] for the outputs of a NSST sensor installed in a motor bondline are reasonable.

Three of the prototype NSST's were calibrated using the NSST calibration rig. The normal calibration factors ranged 0.37 to 0.43 mV per N (0.16 to 0.19 mV per kPa or 1.12 to 1.30 mV per psi). The shear calibration factors ranged from 0.10 to 0.13 mV per N (0.04 to 0.06 mV per kPa or 0.30 to 0.39 mV per psi).

8. FUTURE WORK

The goal of Micron Instruments is to commercialize the Normal Shear Stress and Temperature (NSST) sensor and make it available to the solid rocket motor community for research and production purposes. The following activities are steps that will contribute to raising the NSST sensor's Technology Readiness Level to 9:

a) Replace the magnetic wire leads with a flex circuit to increase robustness and simplify installation.

b) Install servo motors on the calibration rig linear actuators and control them with a closed-loop force controller. A programmable controller would allow simultaneous application of force increments to maintain the steady boundary conditions in the Y (shear) and Z (normal) directions.

c) Manufacture an increased quantity of NSST sensors, calibrate them and evaluate the statistical variability of the calibration factors and crosstalk. These results will guide the refinement of the NSST manufacturing process.

d) Design a wireless, passively powered data transceiver on a case/liner/propellant-compatible flex circuit for the NSST sensor. An integrated NSST sensor patch will facilitate its installation and simplify data measurement in a rocket motor production line as well as in a storage environment.

9. REFERENCES

[1] Francis, EC, Thompson, RE, (1982), "Solid propellant stress transducer design and stability data", 28th International Instrumentation Symposium, Instrument Society of America.

[2] Fillerup, J.M., Wong, F.C., (2020), "Development of a Normal Shear Stress and Temperature (NSST) Sensor for Solid Rocket Motor Health Monitoring – Finite Element Analysis and Data Reduction", Micron Instruments, Micron CR 2020-001, February 2020.

[3] Physik Instrumente, https://www.pi-usa.us/fileadmin/user_upload/pi_us/files/product_datasheets/H825_Medium_Load_Hexapod_datasheet.pdf, accessed March 1, 2020.

[4] http://www.nookindustries.com/Product/ProductLine/Screw-Driven-Modular-Actuators, accessed 24 April 2020.

[5] http://www.nookindustries.com/Product/ProductName/100546/ELK%2030, accessed 24 April 2020.

[6] https://www.interfaceforce.com/products/multi-axis-sensors/3axx-3-axis-force-load-cell/, accessed 27 April 2020.

[7] http://www.nookindustries.com/EngineeringTool/Index, accessed 24 April 2020.

[8] http://www.nookindustries.com/Content/media/NOOK-Modular-Linear-Actuator-Catalog.pdf, accessed 27 April 2020.

[9] https://mecway.com/, accessed 27 April 2020.

[10] http://innomet.ttu.ee/martin/mer0070/loengud/fea_best_practices.pdf, accessed 27 April 2020.

[11] https://www.mcmaster.com/1372n42, accessed 29 April 2020.

[12] https://pdfs.semanticscholar.org/fd92/37048177e09eed0ac43e1b337f18e84de116.pdf, accessed 29 April 2020.

[13] https://www.cati.com/blog/2011/07/convert-durometer-to-youngs-modulus/, accessed 29 April 2020.

[14] https://www.sealseastern.com/pdf/shore-a%20durometer%20and%20engineering%20properties.pdf, accessed 29 April 2020.

[15] https://www.mcmaster.com/3427a23, accessed 29 April 2020.

[16] https://www.echotape.com/products/dc-k048a-strong-double-sided-tape-temporary/, accessed 28 April 2020.

[17] https://www.echotape.com/products/dc-m012p-clear-double-sided-mounting-bonding/, accessed 28 April 2020.

[18] https://www.echotape.com/products/dc-u032a-white-double-sided-tape-mounting-bonding/, accessed 28 April 2020.

[19] https://3m.citrination.com/pif/000296?locale=en-US, accessed 28 April 2020.

[20] Hoffman, K., "Applying the Wheatstone Bridge Circuit", http://eln.teilam.gr/sites/default/files/Wheatstone%20bridge.pdf, accessed 21 Sep. 2017.

[21] https://www.tek.com/keithley-source-measure-units/keithley-smu-2400-series-sourcemeter, accessed 27 June 2020.

[22] https://www.tek.com/keithley-switching-and-data-acquisition-systems/keithley-daq6510, accessed 27 June 2020.

[23] https://www.interfaceforce.com/products/digital-instrumentation/signal-conditioners-digital-instrumentation/bsc4d-multi-channel-bridge-amplifier-and-pc-interface-module/, accessed 27 June 2020.

ANNEX A – COMPONENT DETAILS AND DRAWINGS

This Annex details the geometry of the support structures used in the NSST calibration rig and the linear actuator specifications.

Nook Industries ELK 30 Actuator Specifications

Part Number: MA-311592-1
Specification: ELK-30/1/000/000/280
Description
Net travel = 110 mm
Absolute travel = 160 mm
Carriage version = 0
Drive version = 0
Ballscrew 8x2.5
Accuracy 0.05 mm/300 mm axial play 0.04 mm
Accessories: Mounting blocks (2), Handwheel (1), Spindle clamp (1), Counter (1)

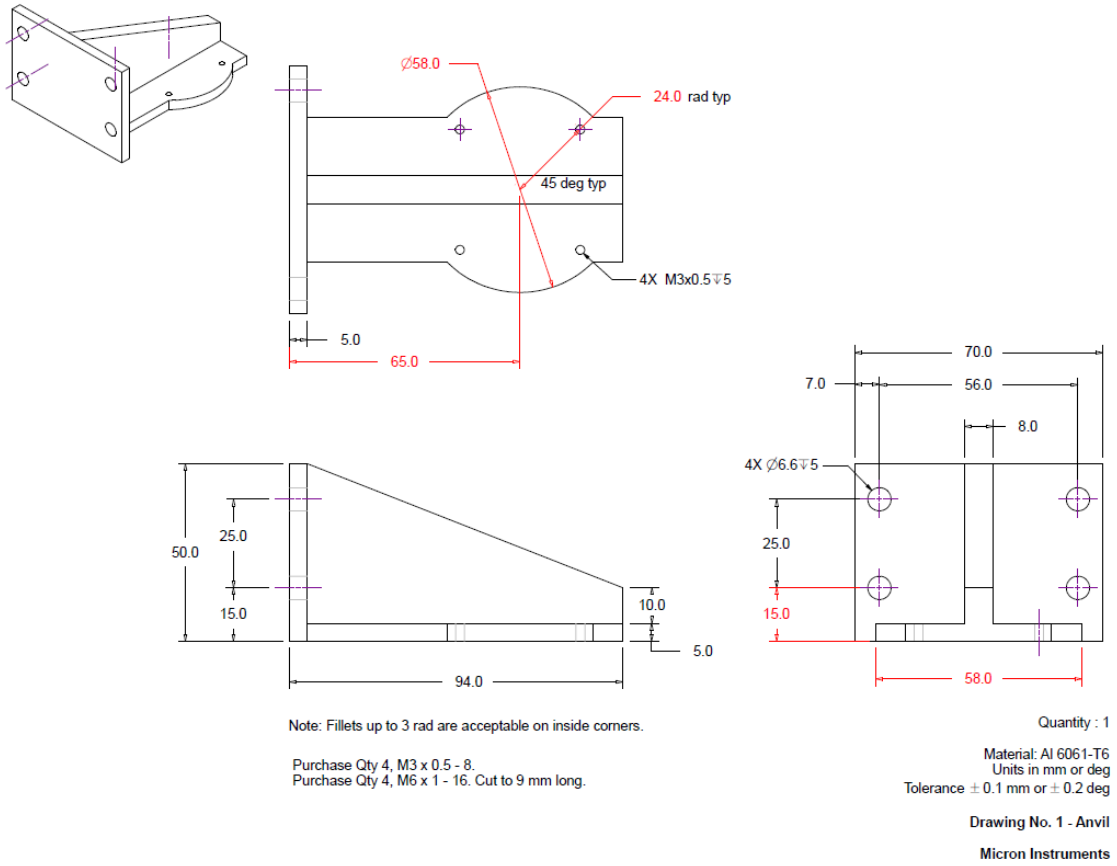

Figure A.1: Anvil

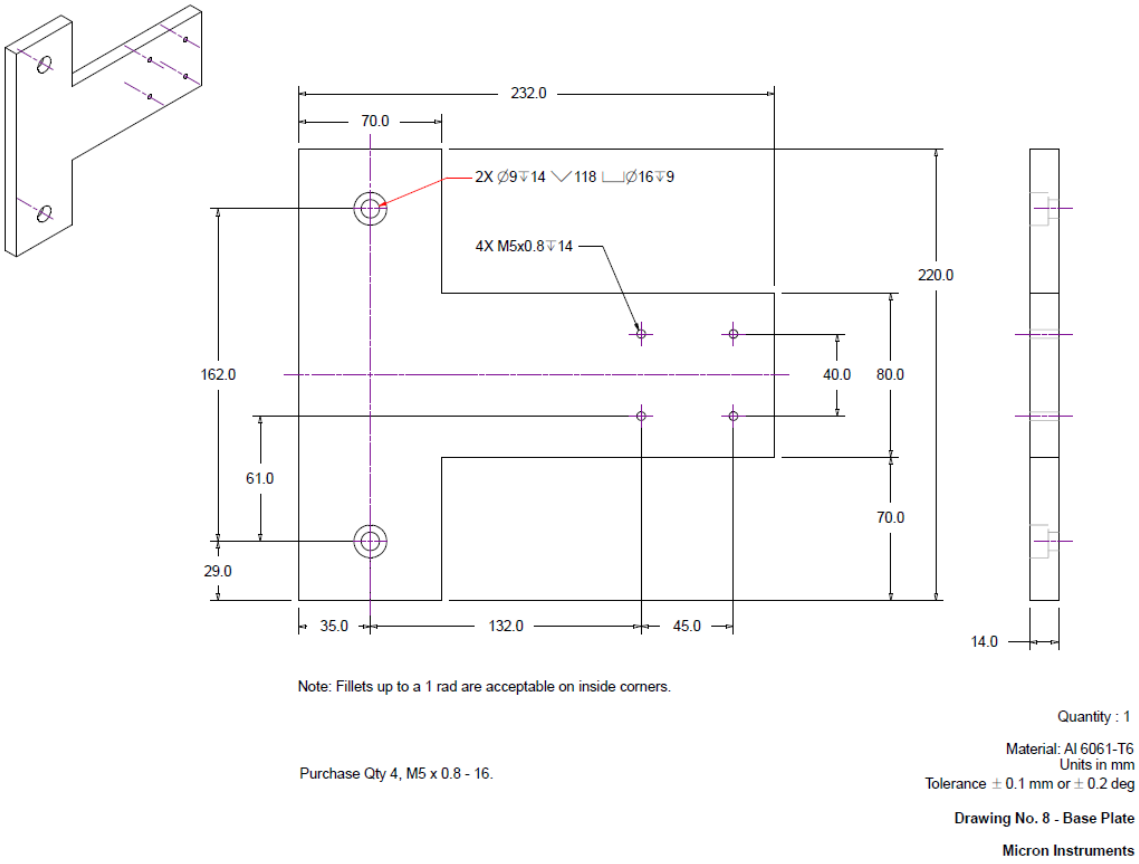

Figure A.2: Base Plate

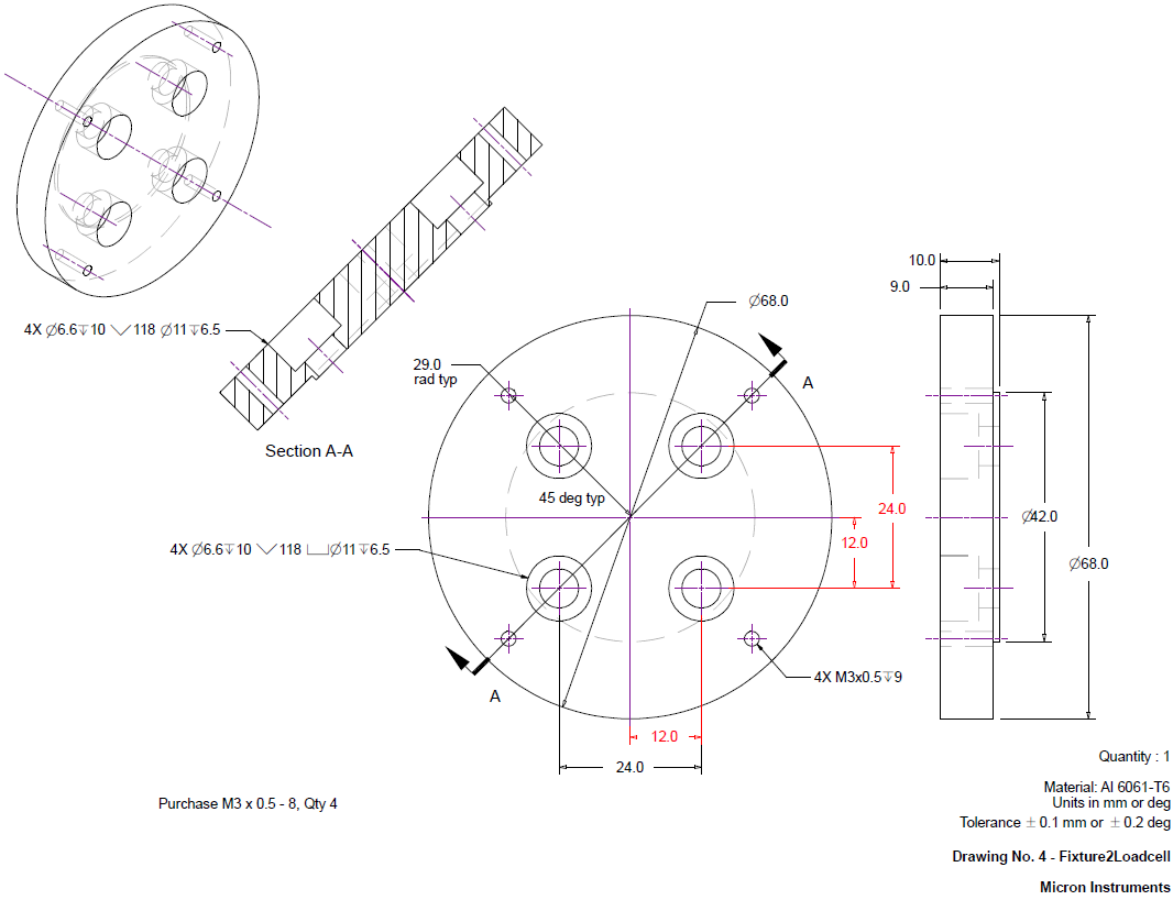

Figure A.3: Fixture to Loadcell Plate

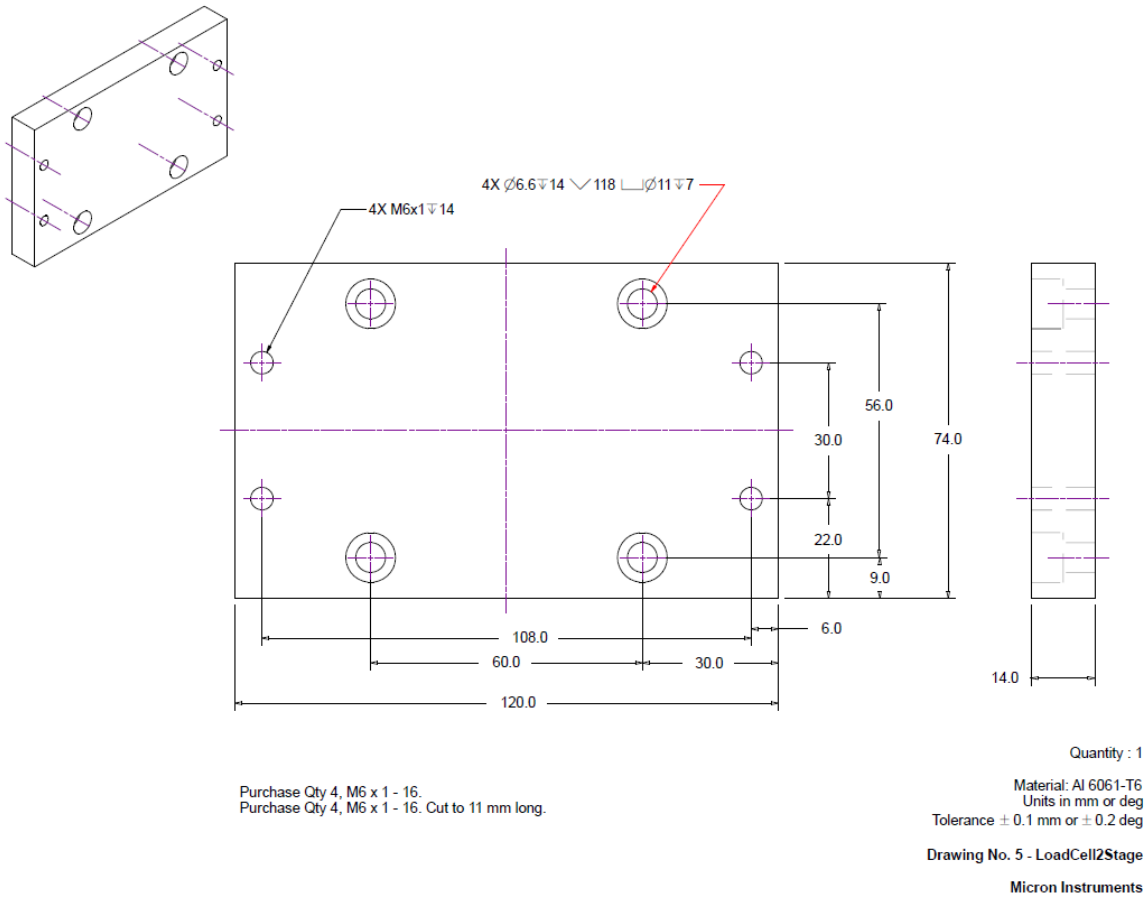

Figure A.4: Loadcell to Stage Plate

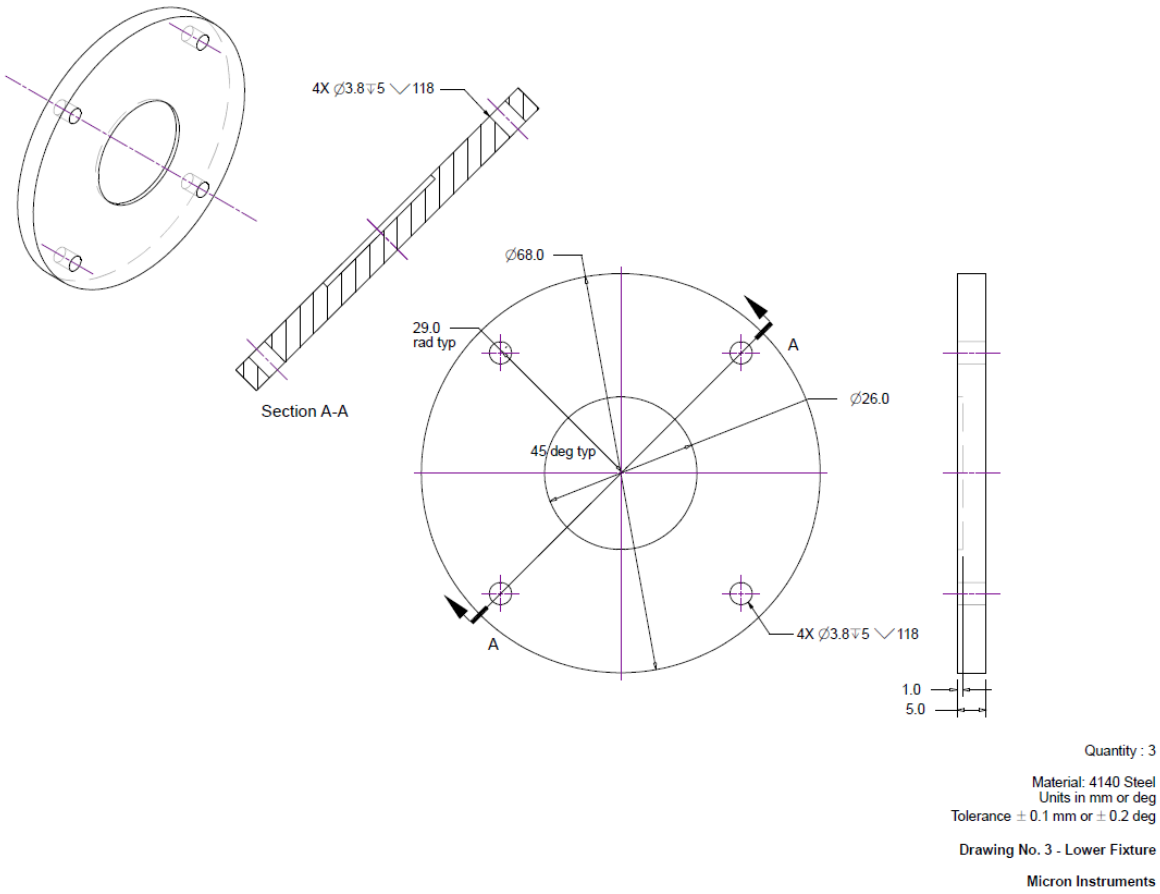

Figure A.5: Lower Fixture

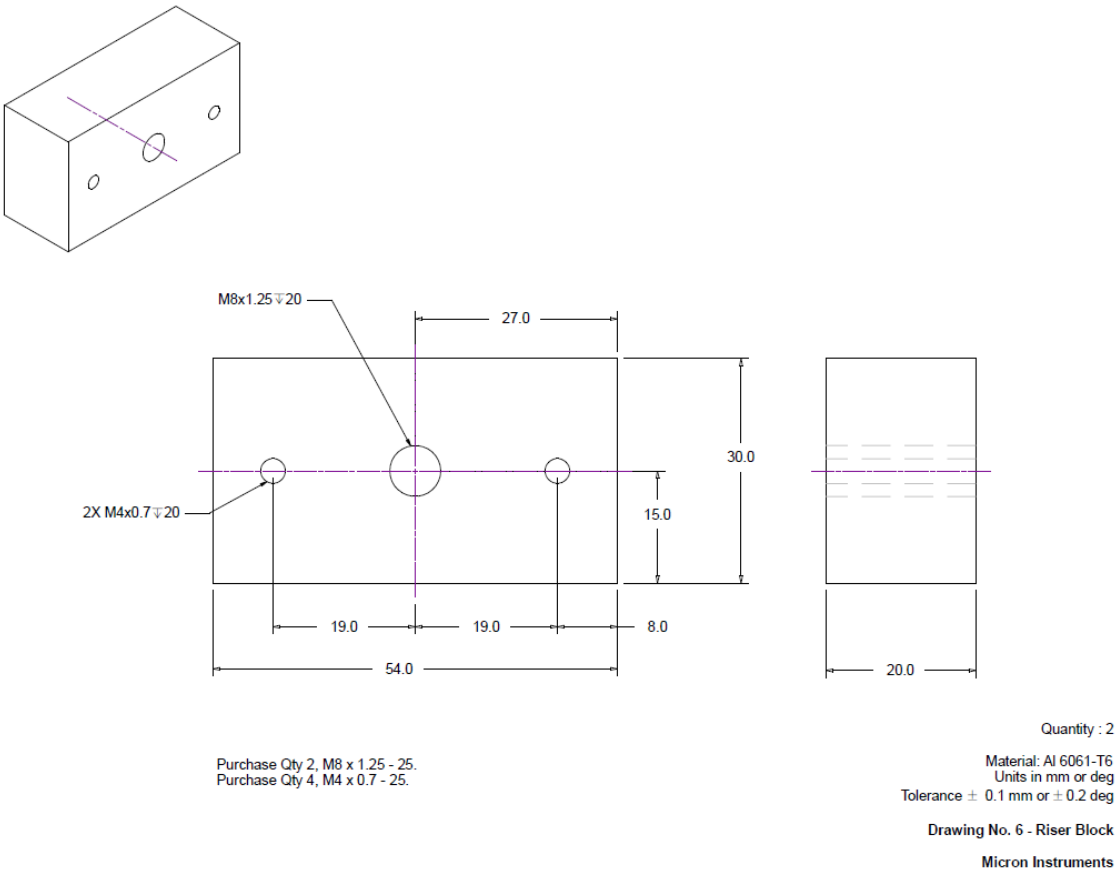

Figure A.6: Riser Block

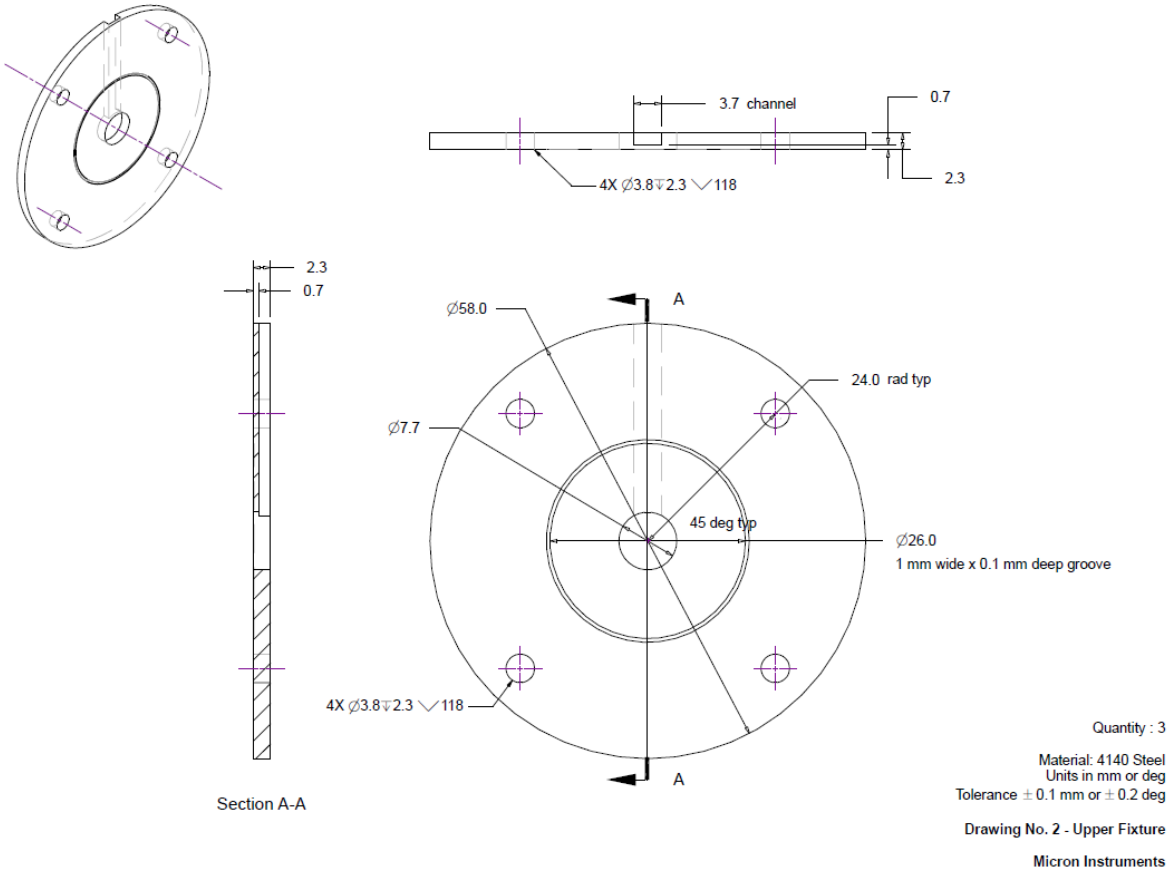

Figure A.7: Upper Fixture

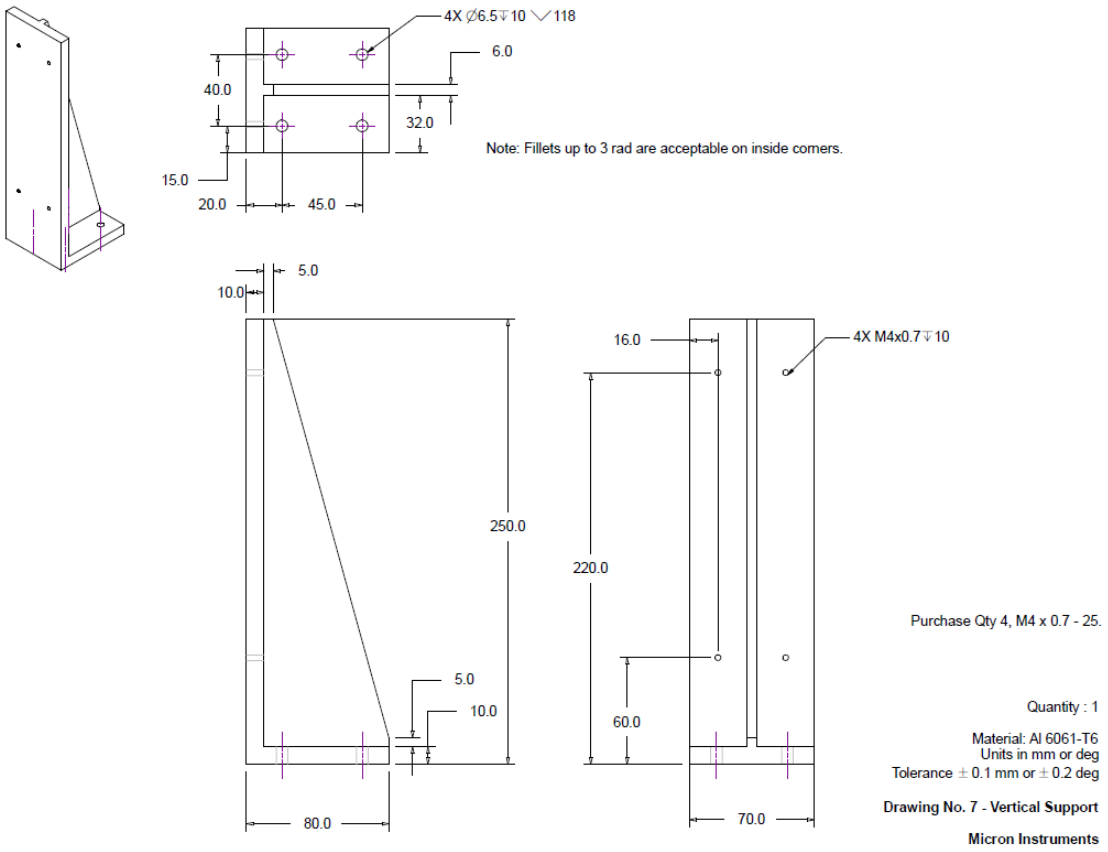

Figure A.8: Vertical Support

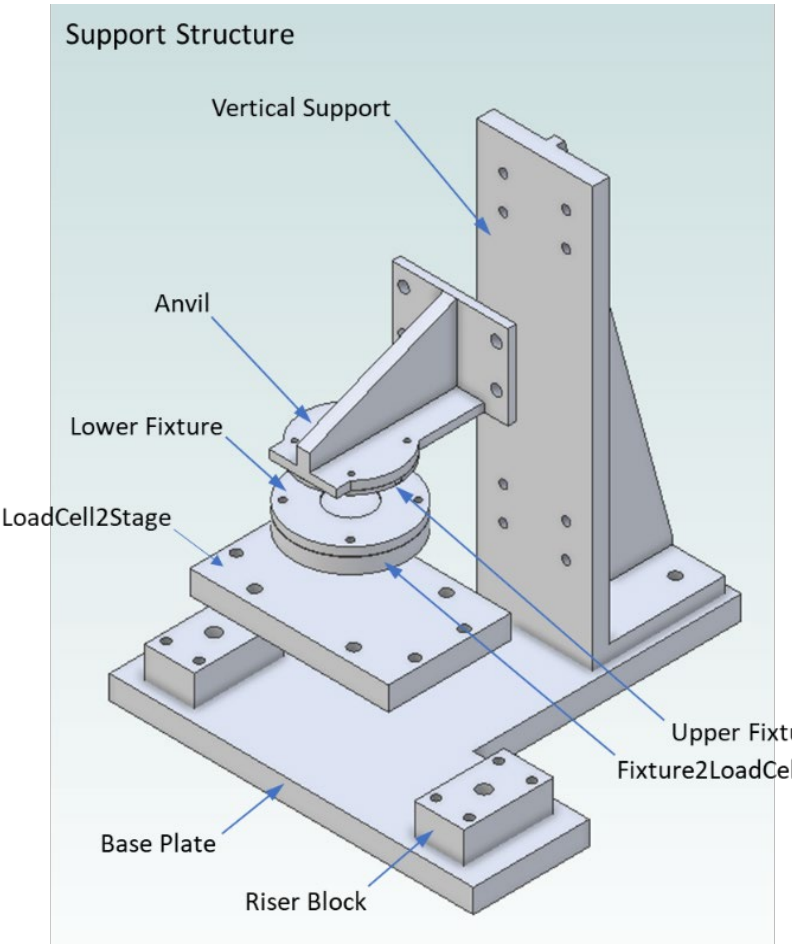

Figure A.9: Support Structure Sub-Assembly

ANNEX B – NSST FIXTURE MOUNTING AND DEMOUNTING

This Annex details the steps to mount and demount the NSST sensor from the NSST fixture.

B.1 Mounting the NSST Sensor

1.1 Turn on the 3-axis load cell data acquisition system and the Keithley multimeter and power sources. Set the power sources to supply 4 mA.

1.2 Take a reading of the NSST normal and shear outputs while the sensor is unmounted.

1.3 Degrease the lower fixture, upper fixture, neoprene cylinder and the sensor diaphragm surfaces.

1.4 Lay the upper fixture on its back with the sensor channel leading to the right.

1.5 Lift up the upper fixture and insert the NSST sensor into the cavity.

1.6 Apply a 25 x 25 mm square of 3M 9832 on the center of the upper fixture.

1.7 Lightly press the 3M 9832 onto the diaphragm and the upper fixture to bond it.

1.8 Lower the neoprene cylinder onto the 3M 9832 ensuring that it is centered on the upper fixture. The NSST normal output should be within 3 mV of the unmounted reading. The NSST shear output should be within 0.3 mV of the unmounted reading.

1.9 Apply a 25 x 25 mm square of EchoTape DC-032A on the center of the lower fixture and remove the topside backing strip to expose the adhesive surface.

1.10 Lightly bolt the upper fixture with the NSST sensor to the anvil.

1.11 Lightly bolt the lower fixture to the loadcell fixture.

1.12 Lower the anvil until the neoprene cylinder almost touches the lower fixture.

1.13 Adjust the Y-stage position so that the neoprene cylinder is centered laterally on the lower fixture.

1.14 Adjust the positions of the upper and/or lower fixtures in the X-direction so that the neoprene cylinder is centered on the lower fixture. Tighten the lower fixture bolts.

1.15 Lower the anvil so that a 100 N compressive force is applied. Hold for 10 s.

1.16 Raise the anvil and adjust the Z-stage position and the Y-position so that there is no load on the NSST sensor.

1.17 The NSST sensor is ready to be calibrated. See Figure B.1 for the completed fixture.

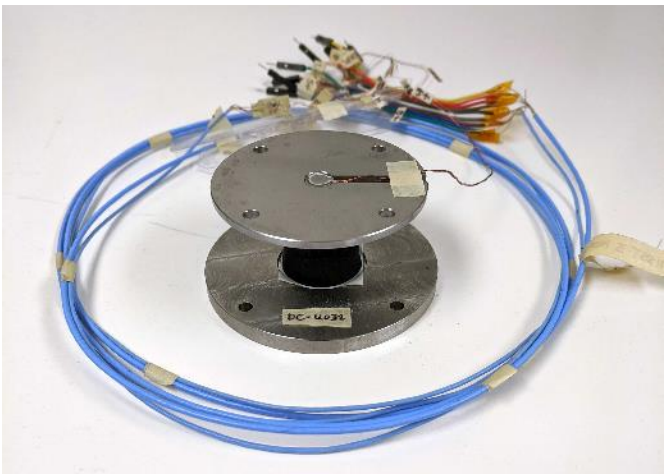

Figure B.1 : Completed NSST Fixture

B.2 Demounting the NSST Sensor

2.1 Bring the Y-stage and Z-stage to a position where there is no load on the NSST sensor.

2.2 Unbolt the upper fixture.

2.3 Unbolt the lower fixture.

2.4 Remove the NSST fixture from the calibration rig.

2.5 Hold the upper fixture in one hand and the lower fixture in the other hand. Make sure the NSST sensor cable is out of the way.

2.6 Twist the lower fixture without applying a normal load on the upper fixture to shear the neoprene cylinder from the 3M 9832 tape. The 9832 backing should remain intact and on the upper fixture. Look at the NSST sensor outputs using the Keithley multimeter to verify that the sensor diaphragm has not been overstressed.

2.7 Peel the 9832 backing off the upper fixture without pulling up on the NSST sensor. Look at the NSST sensor outputs using the Keithley multimeter to verify that the sensor diaphragm has not been overstressed.

2.8 Disconnect the NSST sensor from the Keithley multimeter and power sources.

2.9 Hold the neoprene cylinder in one hand and the lower fixture in the other hand.

2.10 Twist and pull on the neoprene cylinder to remove it from the DC-032A tape.

2.11 Peel the DC-032A tape from the lower fixture.

2.12 Use a solvent to remove the 9832 and DC-032A tape residue from the upper fixture, lower fixture, neoprene cylinder and sensor diaphragm surfaces.

LIST OF ACRONYMS

AMRDEC.	U.S. Aviation and Missile Research Development and Engineering Center
DBST	Dual Bond Stress and Temperature sensor
FEA	Finite Element Analysis
NSST	Normal-Shear Stress and Temperature sensor
SRM	Solid Rocket Motor

This page intentionally left blank.